
RESPONSE TO REQUEST FOR ADDITIONAL INFORMATION

3/24/2014

US-APWR Design Certification

Mitsubishi Heavy Industries

Docket No. 52-021

RAI NO.: NO. 1060-7285 REVISION 4
SRP SECTION: 03.07.02 – Seismic System Analysis
APPLICATION SECTION: 3.7.2
DATE OF RAI ISSUE: 11/15/2013

QUESTION NO. 03.07.02-233:

Part 1

The soil-structure interaction (SSI) and structure-soil-structure interaction (SSSI) models described in the technical report MUAP-10006, "Soil-Structure Interaction Analysis and Results for the US-APWR Standard Plant," Revision 3, include solid brick elements connecting the free field soils and the basement structural elements, in order to simulate the near field backfill material that is expected to surround the structures. In the case of the SSSI analysis, backfill elements are also utilized in the volume between the Reactor Building (R/B) Complex and Turbine Building (T/B) basements. These backfill elements are shown in Figures 03.3.4.1-4, "R/B Complex with Backfill Soil Elements," through 03.3.4.2-3, "SSSI Model with Backfill and Free Field Soils (Looking East)."

The applicant is requested to provide the following additional information related to modeling of backfill:

(1) Tables 03.3.1-8, "Backfill Small-Strain Properties for Profiles 270-200, 270-500 and 560-500," and 03.3.1-9, "Backfill Small-Strain Properties for Profiles 900-100, 900-200 and 2032-100," indicate small-strain P-wave velocities between 1350 ft/s and 2500 ft/s, which implies the backfill is not saturated. Since the SSI analysis assumes saturated conditions for the free field soils up to grade elevation, explain the technical basis for the unsaturated assumption for the backfill. Revise MUAP-10006, Revision 3, to address this inconsistency.

(2) Clarify whether stresses in the backfill elements, as computed from the SSI analysis, are used to estimate dynamic soil pressures for design of embedded walls. If this is not the case then revise MUAP-10006, Revision 3, to add this clarification.

(3) Revise DCD Section 3.7 to be consistent with the revisions to MUAP-10006, Revision 3, indicated in items (1) and (2) above.

Part 2

The guidance in SRP 3.7.2, Revision 3, SRP Acceptance Criterion 4, "Soil Structure Interaction," indicates that sensitivity studies should be performed to identify the effects of potential separation of soil from sidewalls, to assist in judging the adequacy of the SSI analysis results. Similar guidance is indicated in the ASCE 4-98 standard.

MUAP-10006, Revision 3, does not include results of such sensitivity studies. Therefore, the applicant is requested to provide the results of sensitivity studies performed to investigate the effect of potential separation of the lateral soil from the embedded sidewalls of the R/B Complex. The results should be provided in terms of transfer functions and In-Structure Response Spectra (ISRS) at key locations throughout the structure.

ANSWER:

Part 1

- (1) The backfill with limited boundary conditions (not infinity) is simulated directly as part of structure using solid brick elements in Soil-Structure Interaction analysis. The material elastic properties of the backfill structural elements, i.e., the Young's modulus and Poisson's ratio, are defined and calculated using strain compatible shear wave velocity (V_s) and compressional wave velocity (V_p). The presence of backfill as simulated in the SSI model has no effect on the input control motions and site response analysis for which the free field soils are used as input. The last paragraph of Section 0.3.3.1, MUAP 10006 Rev.3 discusses the approach used to determine the elastic material properties for the backfill elements. Table 3.3.1-8 and Table 3.3.1-9 of MUAP 10006 Rev.3 list the properties, small strain V_s , V_p along with other properties for the two sets of backfills. The small strain Poisson's ratios are 0.35 and 0.30 for backfills represented by Table 3.3.1-8 and Table 3.3.1-9, respectively. These Poisson's ratios are the commonly used values for granular soils (See tables in page 123 of Foundation Analysis and Design, Fifth edition, by Joseph E. Bowles). The Poisson's ratio with values other than approaching 0.5 represents the soil-water-void system will experience significant volume changes under compressive loadings, or a drained condition for the soil-water-void system. The use of small strain properties listed in Table 3.3.1-8 and Table 3.3.1-9 of MUAP 10006 Rev.3 and associated strain compatible backfill soil properties is intended to consider possible scenario with drained condition for the saturated backfills during earthquake excitations.

A sensitivity study was performed to investigate the effect of Poisson's ratio of the backfill on the structural response at various key locations of the Reactor Building (RB) Complex. The study is described as follows:

(a) Study Model

The study was performed based on an in-progress version of the R/B complex structure, referred to as study model herein, that consisted of prestressed concrete containment vessel (PCCV), containment internal structure (CIS), east and west power source buildings (PS/Bs), auxiliary building (A/B) supported on a common basemat. Along with minor differences on thickness of some walls, the major difference between this in-progress version of R/B complex and the final R/B complex documented in Technical Report MUAP-10006 Rev. 3, referred to as final model herein is that the in-progress version doesn't include the essential service water pipe chase (ESWPC). Integrating ESWPC only represents less than 10% increase of the foundation size in plant north to south direction while foundation embedment depth and foundation size in east to west direction are the same for the two versions. Therefore, the differences do not compromise the conclusion of the study.

The study model and final model share the same finite element discretion of the structure, except that the study model includes one row of backfill elements surrounding the structure while the final model has two rows of the backfill elements. Stiffness associated with uncracked concrete was assigned to the structural elements of the study model. The development of the study model followed the same criteria and used the same approach as the ones described in Section 2 of MUAP 10006 R3 for the final model. The study model including structural and backfill soil elements are shown in Figure 1. The excavated volume is shown in Figure 2. Figure 3 shows the backfill solid elements alone.

(b) Soil Profile and Input Backfill Properties

The study was performed for the generic soil profile 560-500 that is documented in MUAP 10006 Rev.3. To investigate the effect of Poisson's ratio of the backfill soils on seismic response of the structure, two cases with different backfill properties are analyzed. Table 1 presents Case 1 strain compatible backfill soil properties that are developed from small strain properties as listed in Table 3.3.1-8 with small strain Poisson's ratio of 0.35. Table 2 presents Case 2 strain compatible soil properties. The only difference between Table 1 and Table 2 is that the compressional wave velocities (V_p) in Table 2 for the backfills are 5000 ft/sec, which is the V_p for compressive wave propagated in water. The resulting Poisson's ratios for Case 2 vary from 0.486 to 0.490. It is corresponding to the condition of saturated soft soil with negligible volume change when subjected to compressive loads.

(c) Study Results and Conclusion

SSI analyses were performed on the two cases using the same methodology and procedures as described in MUAP 10006 Rev.3 for final production runs. The Acceleration Response Spectra (ARS) of selected nodes at critical locations were developed and compared for the two cases. The critical locations are the top of reactor cavity, the sump strainer, the spent fuel pool, the new fuel storage pit, the Gas Turbine Generator A (GTG A) in east PS/B, and GTG B in west PS/B. One node per critical location was selected to develop ARS. The rule of Square Root of the Sum of Squares (SRSS) was used to combine co-directional responses to develop the ARS. Figure 4 through Figure 21 present the ARS developed for the critical locations. In the figures, the case 1 ARS is represented by the black solid line and the pink solid line denotes the case 2 ARS.

Negligible differences are observed in the horizontal directional responses for the critical locations. This is because the two cases have the same shear wave velocities for the backfill elements. Small differences, with Case 1 responses being higher than Case 2 responses, were observed in the vertical response as shown on Figures 15, 18, and 21 for the New Fuel Storage Pit, GTG A and GTG B, respectively.

Based on the study, it is concluded that use of Poisson's ratios for the backfill elements corresponding to soils under drained condition are appropriate for the SSI analysis of US-APWR standard plant R/B Complex. Clarification will be added to MUAP 10006 Rev.3 Section 3.3.1 for backfill element elastic properties per study as described above. A calculation package will be developed to document this study.

- (2) The stresses in the backfill elements, as computed from the SSI analysis, are not used to estimate dynamic soil pressures for design of embedded walls. The dynamic

soil pressures for design of the embedded walls are based on Wood's solution (See Figure 3.5-1 of ASCE 4-98) and static passive earth pressures.

(3) Section 3.7 of DCD will be revised per items (1).

Part 2

A sensitivity study on the effect of foundation embedment conditions on the seismic response of the US-APWR standard plant R/B complex was performed on the same structural model as described in Part 1 of this response. SRP 3.7.2 requires investigating “effects of partial separation or loss of contact between the structure (embedded portion of the structure and foundation mat) and the soil during the earthquake.” This study performed SSI analyses on the two bounding embedment condition cases to meet the SRP requirement. The two bounding cases, in terms of contact between the basement walls and the side soils, are as follows:

- Unbonded embedment, also referred to as “0-sided” embedment. No connectivity (unbonded) is assumed between the basement perimeter walls and the lateral soils. It represents that the walls have no restraints from the lateral soils and the walls and the side soils are fully separated during seismic excitations, therefore there is no direct load transfer between the walls and the side soils during the earthquake excitation.
- Fully bonded embedment, also referred to as “4-sided” embedment. The basement perimeter walls are fully bonded with the side soils in the four sides of the building. In this case, there will be interaction between the side soils and the basement walls during earthquake excitation.

From the seismic response perspective, embedment of a structure by the surrounding side soil medium generally produces two associated effects depending on the embedment conditions:

- (a) Changes in the frequency-dependent foundation impedances which can result in shift in the SSI system frequencies and changes in associated SSI system damping values.
- (b) Effect on seismic response of the structure due to seismic response of the side soil layer which can in turn result in variations in the SSI system seismic response Transfer Function (TF).

These two bounding cases, unbonded and full bounded, are expected to reveal the minimal and maximal effects of the aforementioned embedment effect (a), respectively and in turn take into account for the aforementioned effect (b).

The unbonded and fully bonded models in this assessment share the same exact R/B complex structural model with a full stiffness level (Uncracked (UC)), and are only different in how they interact with the surrounding soils. Figure 22 and Figure 23 show the sectional elevation view of the unbounded model and fully bounded model including free field soils, respectively. The fully bonded model uses backfill material elements to connect the basement structure and the surrounding soils. The unbounded model has void between the side free field soils and the basement walls to simulate the separation of the walls and the soils. Since embedment tends to stiffen the system and shift the resonant frequency to a higher value and since uncracked models usually control higher frequency responses than cracked models, the use of the uncracked R/B complex model in this study with the embedment conditions is expected therefore to produce peak responses.

The six generic soil profiles, namely, 270-200, 270-500, 560-500, 900-100, 900-200 and 2032-100, as documented in Technical Report MUAP 10006 Rev.3 Section 2, and

corresponding SSI input soil laying and properties documented in the Section 3 of the Technical Report, are used in this assessment.

The three components of CSDRS compatible time histories used for this study are from an in-progress version of input acceleration time histories but are fully in compliance with requirements of SRP 3.7.1 Option 1, Approach 1. The development of SSI input control motions and elastic material properties for the backfill elements follows the same procedure/methodology as described in Section 3 of the Technical Report. This is the case for SSI analysis methodology/procedure as well.

In order to understand the embedment effects on the R/B complex, Acceleration Transfer Functions (ATF) and the In Floor Response Spectra (ISRS) for the critical locations are compared between the unbonded and fully bonded models. The responses of each model, unbonded and fully bonded combined with the six generic soil profiles are expected to indicate how each of them reacts at various frequencies for different site conditions, ranging from soft soil to hard rock. The maximum base shears obtained from the cases analyzed are also compared to assess the embedment condition effect. The comparisons are discussed as follows

(1) Embedment Condition Effect – ATF Comparison

The ATF at various critical locations are obtained and compared. The comparisons for ATF's at the top of the reactor cavity are provided in this response as an example. The ATF plots The ATF comparison plots of unbonded (0-sided) embedment versus fully bonded (4-sided) embedment at the top of the reactor cavity are provided in Figure 24 thru Figure 41. Both models present smooth ATF curves with no anomalies. Table 3 provides a comparison of the first peak frequency for all six soil cases at the top of the reactor cavity.

Table 3 Indicates that, at the Reactor Cavity:

- Compared to unbonded model, fully bonded conditions make the soil structure system first horizontal fundamental frequencies at top of the reactor cavity shift to higher frequency value for the soil site 270-500, 270-200 and 560-500. This frequency shift is not observed for the rock site profile 900-100,900-200 and 2032-100.
- The bond/contact conditions have minimal effect on the first vertical fundamental frequency of the system for all six generic soil profiles.
- There are reductions for the horizontal ATF amplitudes at the first peak frequencies comparing the fully bonded model to the unbonded model for all six generic soil profiles.

(2) Embedment Condition Effect –ISRS Comparison

ISRS comparison plots of unbounded (0-sided) embedment versus fully bonded (4-sided) embedment at the six critical locations are presented in Figure 42 through Figure 60. The plotted ISRS are the envelope of the six soil profiles for the uncracked 0-sided and 4-sided model, respectively and with +/- 15% peak frequency broadening according to the procedure described in MUAP 10006 Rev. 3 Section 3.

(3) Embedment Condition Effect – Comparison of Base Reaction Forces

Time history based quasi static base reaction forces; base shear and vertical force for each soil profile and model are calculated according to procedures as follows:

- a) Nodal acceleration time histories of all three directions (NS, EW and vertical) are obtained from post processing the ACS SASSI results. The nodal time histories usually have duration of about 23 seconds and the time step is 0.005 second.
- b) The inertial force time history at each node in each of the three directions is calculated as product of the nodal mass and the corresponding nodal acceleration
- c) Horizontal base reaction force time history in each of the three directions is calculated as a sum of corresponding nodal inertial force from all structural nodes
- d) Maximum base reaction force in each of the three directions is then obtained by taking the maximum value for the entire duration of the time history and presented in Table 4 for both unbonded (0S) and fully bonded (4S) models, and the six generic soil profiles.

As indicated in Table 4, base reaction force results (time history based) show small differences (less than +/- 6%) between the 0-sided and 4-sided embedded models.

(4) Embedment Condition Effect-Conclusion

The results show that the seismic response from the unbonded model is comparable to the response from the fully bonded model. For the ISRS, the unbonded model response generally produces higher accelerations in the low frequency range (0 to 10 Hz) for all three directions, while the fully bonded model generally produces higher accelerations in the high frequency range (10 to 100 Hz) for all three directions. However, this is not the case for all the locations. The expected shift in peak frequencies due to the surrounding side soils of the fully bonded model is evident in most locations, such as the top of the reactor cavity, but is not evident for all locations. Therefore, there is no clear evidence of which embedment condition produces a higher seismic response for the seismic Category I equipments housed in the R/B complex. Due to the comparable seismic results produced by the unbonded and fully bonded cases, it is concluded that either case can be served as an appropriate representation for the US-APWR Standard Plant Reactor Building complex SSI analysis for the six generic soil profiles.

Table 1 Backfill Properties for Case 1

Layer	Thickness (ft)	Vp (ft/sec)	Vs (ft/sec)	Density (kcf)	Damping	Poisson's Ratio
1	5.583	1453.7	684.2	0.125	0.022	0.357
2	5.583	1562.5	719.9	0.125	0.028	0.365
3	7.000	1562.5	692.0	0.125	0.035	0.378
4	5.375	1771.7	793.8	0.125	0.029	0.374
5	5.375	1871.2	828.7	0.125	0.031	0.378
6	6.667	1871.2	833.6	0.125	0.030	0.376
7	6.667	1871.2	823.8	0.125	0.034	0.379

Table 2 Backfill Properties for Case 2

Layer	Thickness (ft)	Vp (ft/sec)	Vs (ft/sec)	Density (kcf)	Damping	Poisson's Ratio
1	5.583	5000.0	684.2	0.125	0.022	0.490
2	5.583	5000.0	719.9	0.125	0.028	0.489
3	7.000	5000.0	692.0	0.125	0.035	0.490
4	5.375	5000.0	793.8	0.125	0.029	0.487
5	5.375	5000.0	828.7	0.125	0.031	0.486
6	6.667	5000.0	833.6	0.125	0.030	0.486
7	6.667	5000.0	823.8	0.125	0.034	0.486

Table 3 First Peak Frequency and its Amplitude Comparison

Soil Case	Direction	Frequency (Hz)			Amplitude		
		0 Sided	4 Sided	Difference (%)	0 Sided	4 Sided	Difference (%)
270-200	North-South	2.20	2.37	-7.79%	1.63	1.54	5.71%
270-200	East-West	2.17	2.37	-8.99%	1.46	1.42	2.83%
270-200	Vertical	2.34	2.29	2.08%	1.50	1.48	1.08%
270-500	North-South	1.71	2.22	-30.00%	1.41	1.28	9.44%
270-500	East-West	1.71	1.86	-8.57%	1.34	1.29	3.82%
270-500	Vertical	2.10	2.10	0.00%	1.14	1.14	0.00%
560-500	North-South	2.69	2.76	-2.71%	1.69	1.58	6.63%
560-500	East-West	2.69	3.00	-11.82%	1.52	1.53	-0.50%
560-500	Vertical	3.71	3.71	0.00%	1.22	1.22	0.00%
900-100	North-South	4.00	4.00	0.00%	2.46	2.27	7.76%
900-100	East-West	3.98	3.96	0.61%	2.19	2.15	1.70%
900-100	Vertical	9.74	9.74	0.00%	2.38	2.38	0.00%
900-200	North-South	3.96	3.98	-0.62%	2.70	2.43	9.78%
900-200	East-West	3.96	3.96	0.00%	2.36	2.28	3.40%
900-200	Vertical	8.74	8.74	0.00%	2.13	2.13	0.00%
2032-100	North-South	4.13	4.13	0.00%	1.86	1.76	5.57%
2032-100	East-West	4.10	4.13	-0.59%	2.02	1.69	16.19%
2032-100	Vertical	10.21	10.21	0.00%	1.79	1.79	0.00%

Table 4 Time History Based Base Reaction Force Comparison

Soil Case	Uncracked								
	NS FX (kips)			EW FY (kips)			Vertical FZ (kips)		
	0S (1)	4S (2)	(2)/(1)	0S (1)	4S (2)	(2)/(1)	0S (1)	4S (2)	(2)/(1)
270-200	347313	357174	102.8%	339558	343976	101.3%	375130	378170	100.8%
270-500	330768	348288	105.3%	323164	340568	105.4%	367202	372539	101.5%
560-500	420123	410861	97.8%	409024	423341	103.5%	359503	367284	102.2%
900-100	505248	485704	96.1%	552244	566850	102.6%	580157	586242	101.0%
900-200	509173	497512	97.7%	505329	521461	103.2%	534615	540145	101.0%
2032-100	482485	466309	96.6%	564097	554684	98.3%	544744	545679	100.2%



Figure 1 Study Model- R/B Complex Structure and Backfill Elements

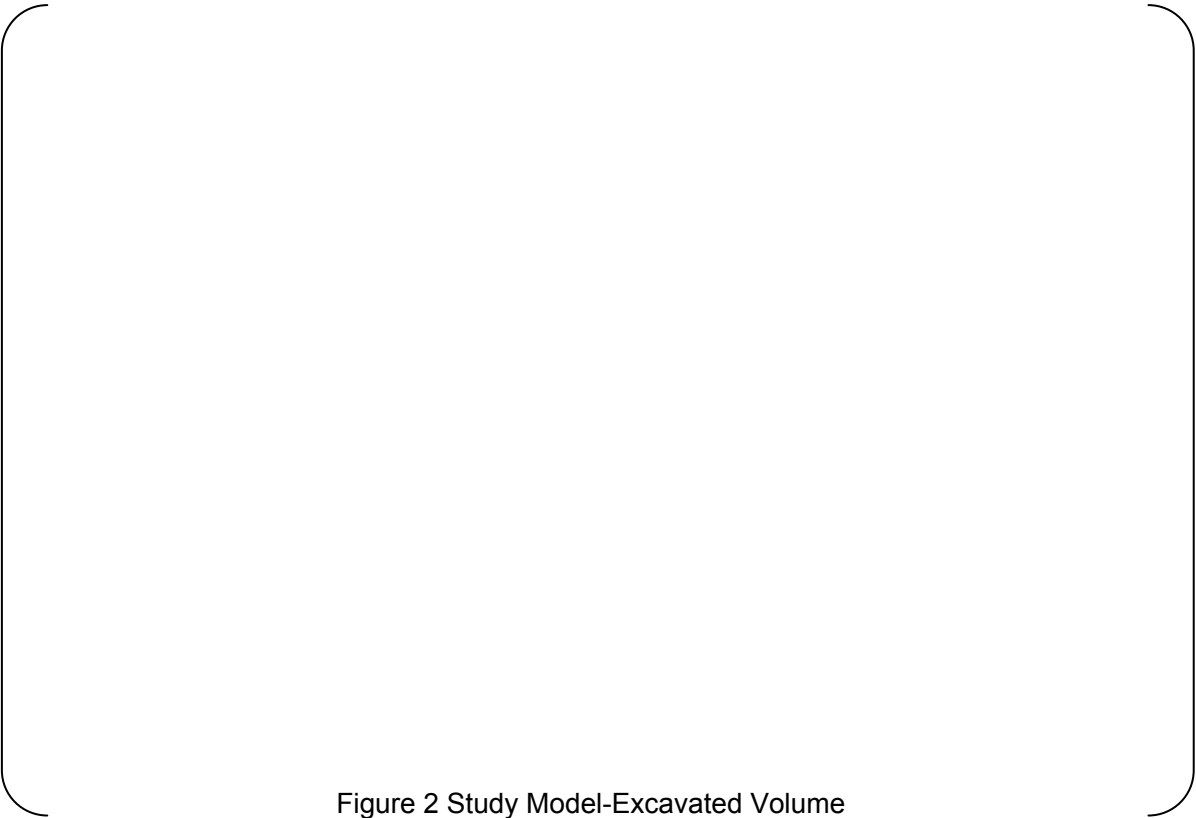


Figure 2 Study Model-Excavated Volume

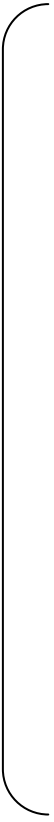


Figure 3 Study Model-Backfill Elements

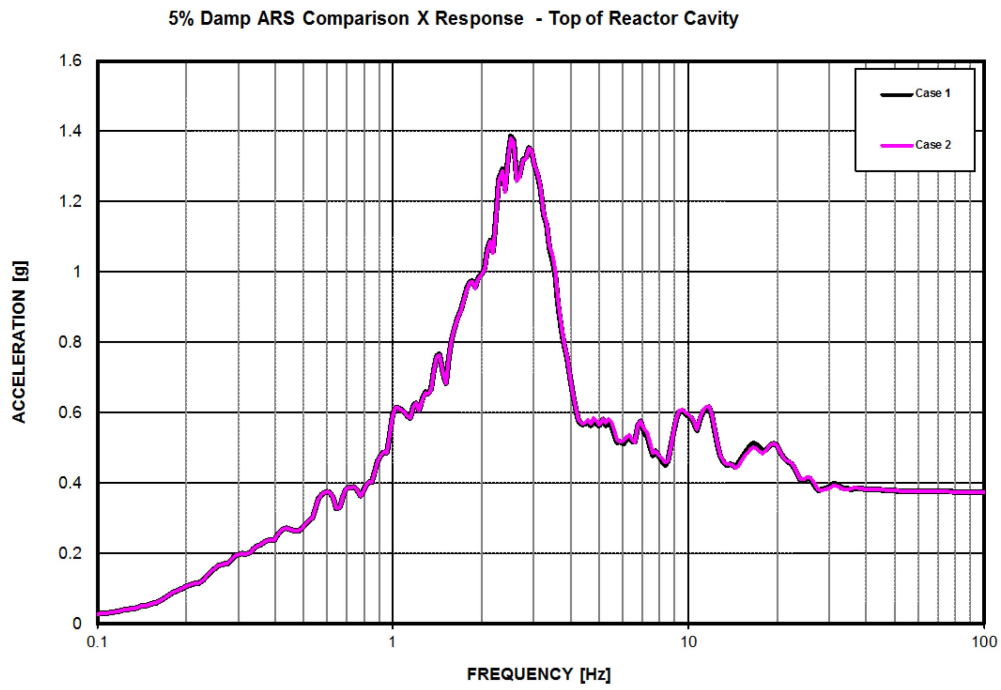


Figure 4 Response in NS direction-Top of Reactor Cavity

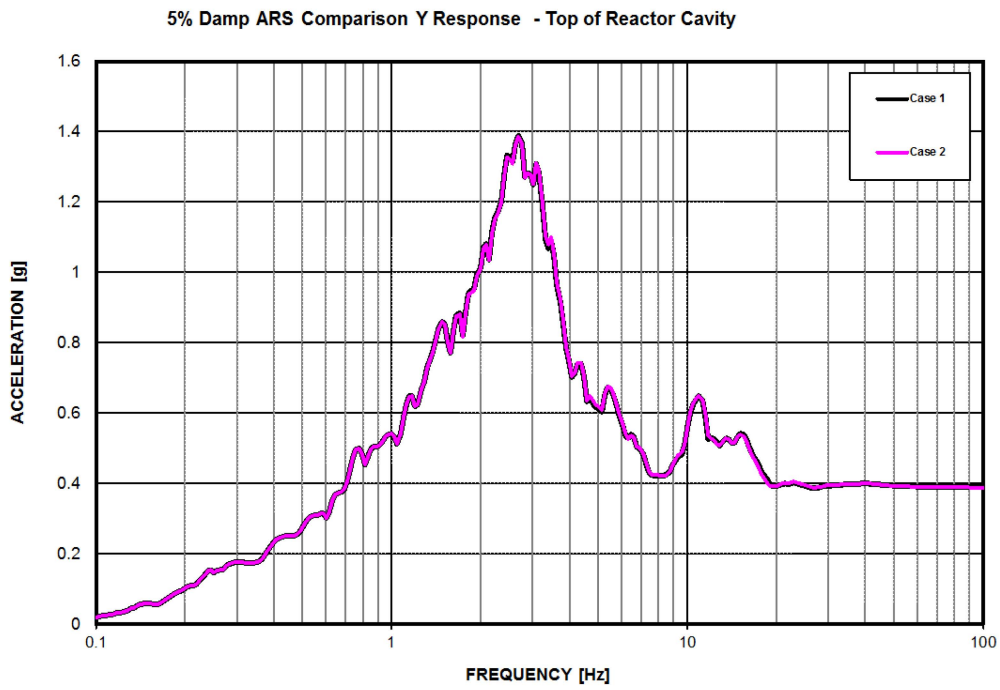


Figure 5 Response in EW direction-Top of Reactor Cavity

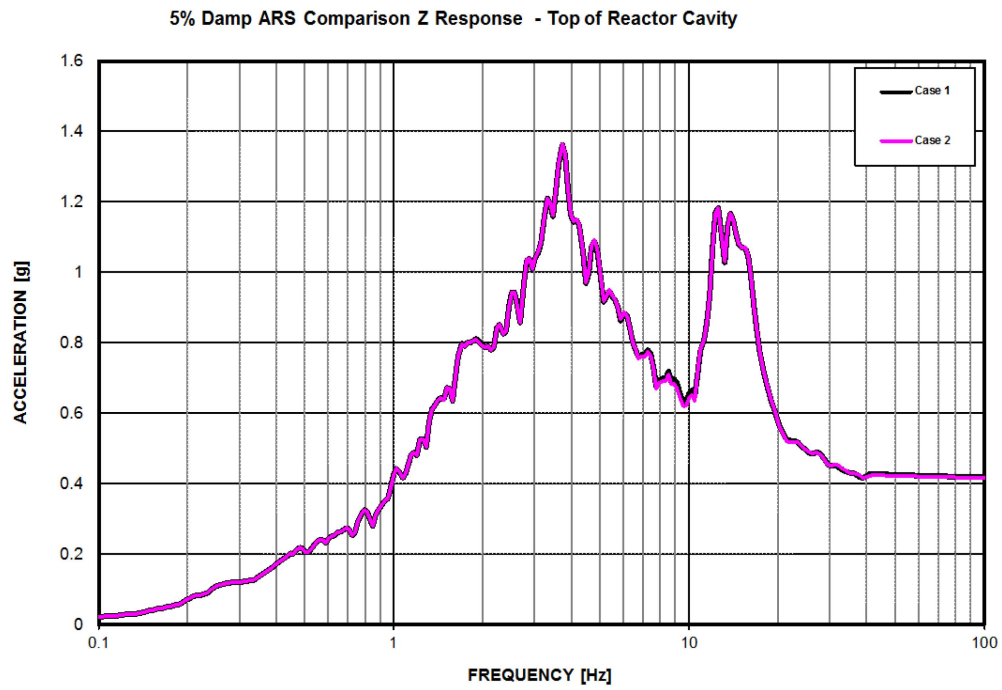


Figure 6 Response in Vertical direction-Top of Reactor Cavity

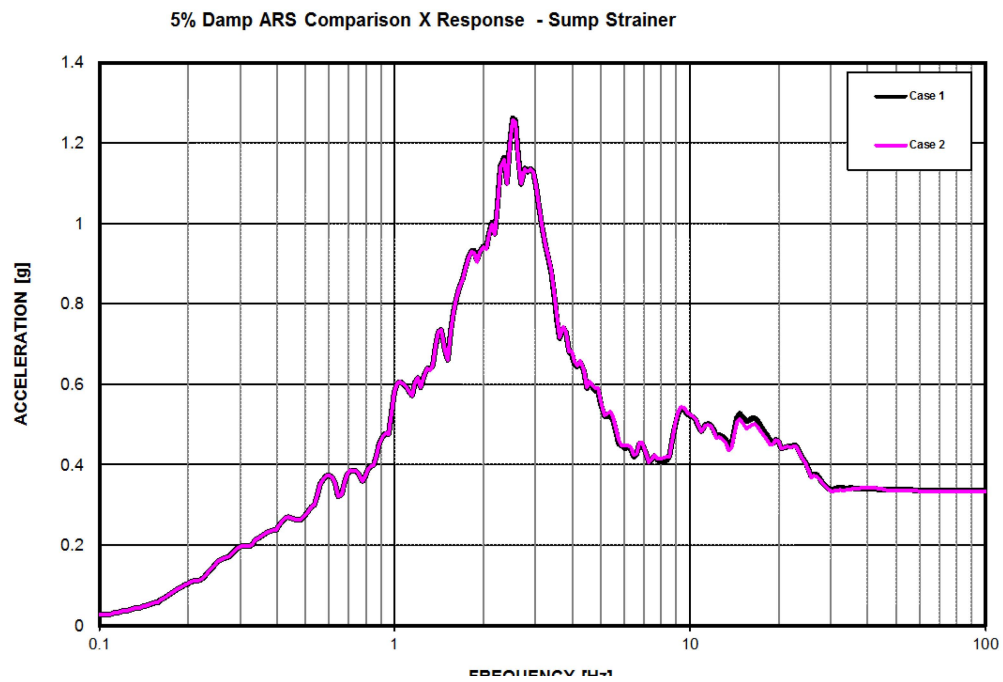


Figure 7 Response in NS Direction-Sump Strainer

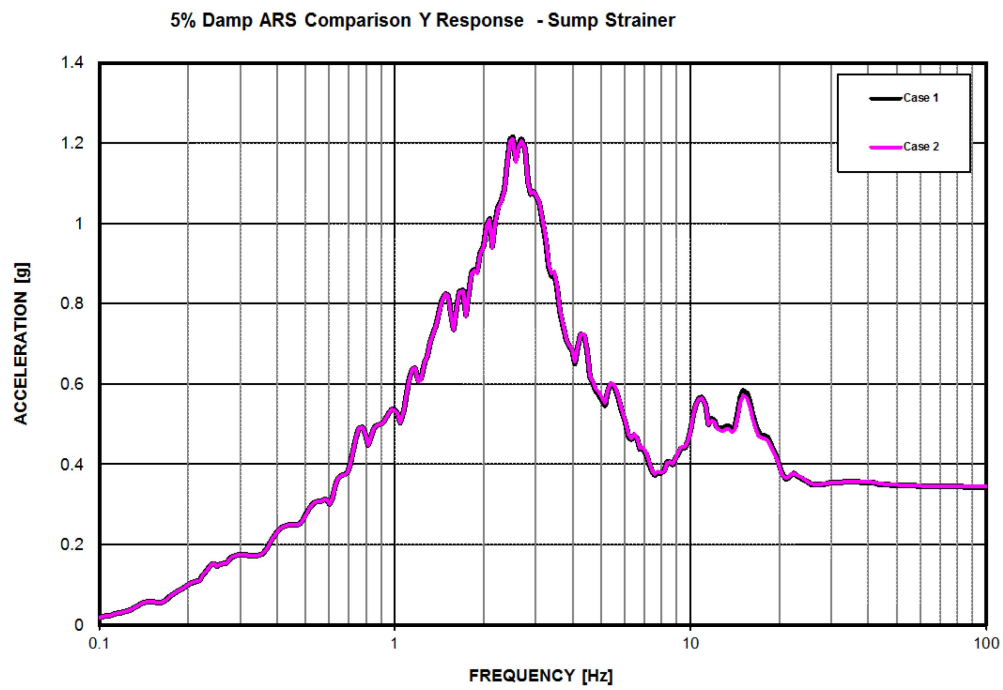


Figure 8 Response in EW Direction-Sump Strainer

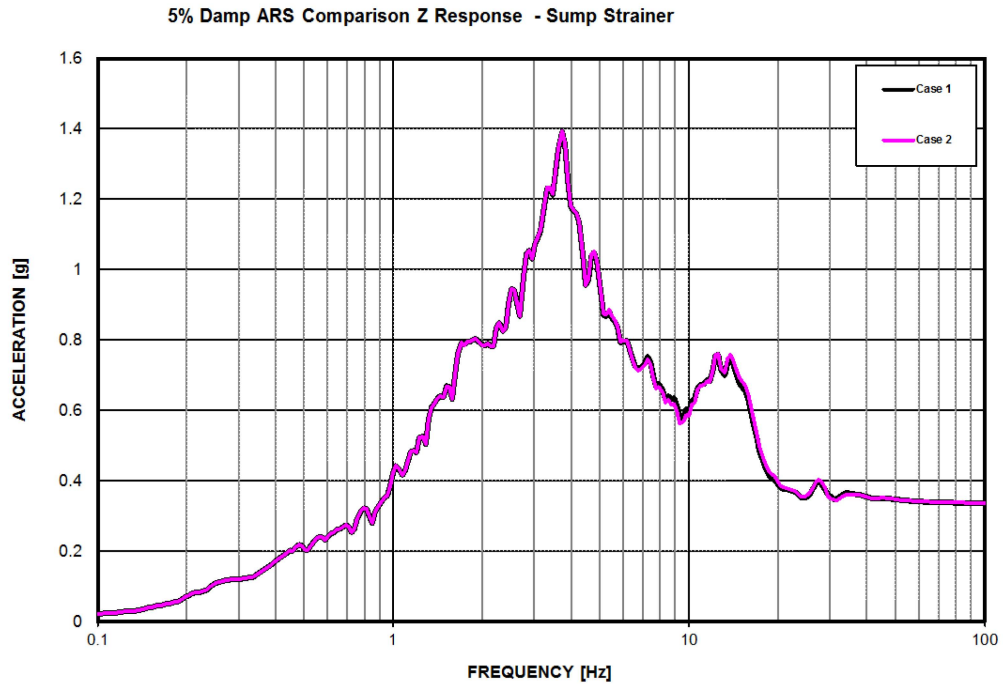


Figure 9 Response in Vertical Direction-Sump Strainer

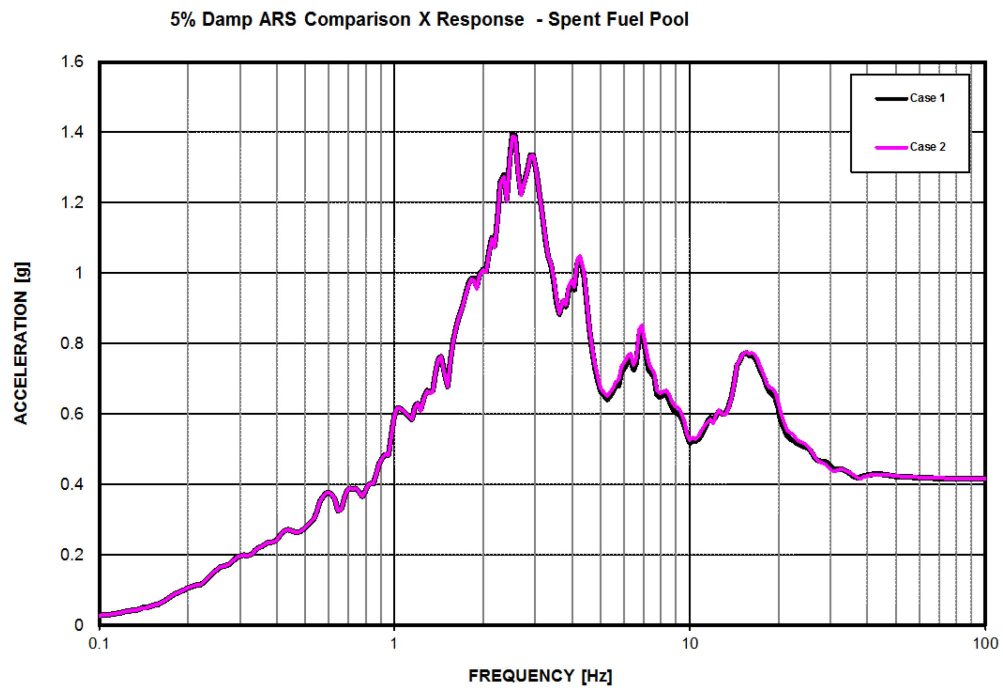


Figure10 Response in NS Direction-Spent Fuel Pool

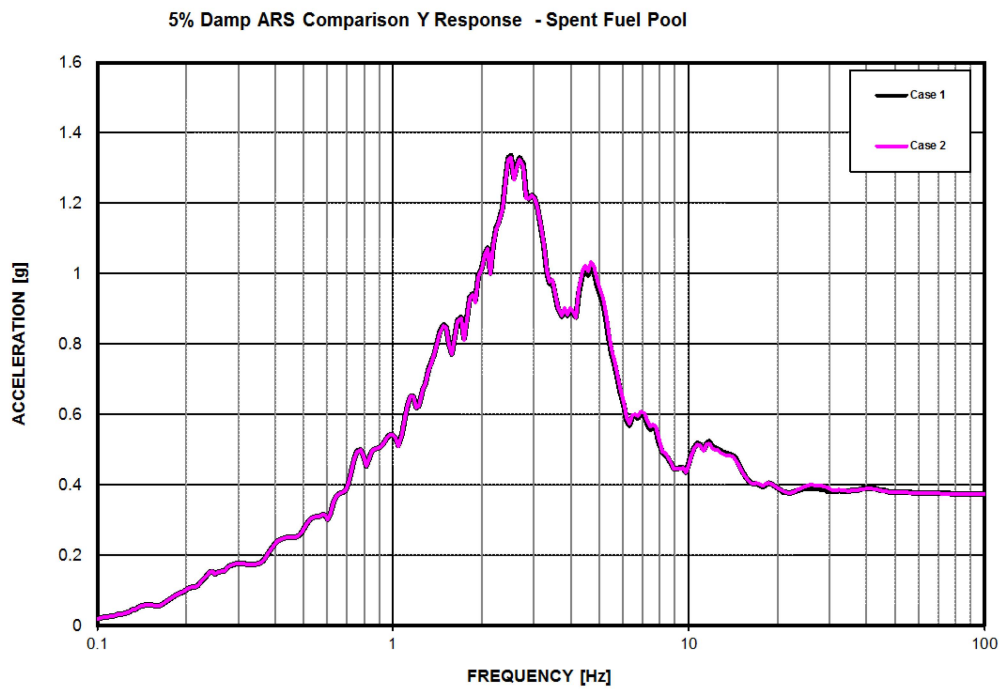


Figure 11 Response in EW Direction-Spent Fuel Pool

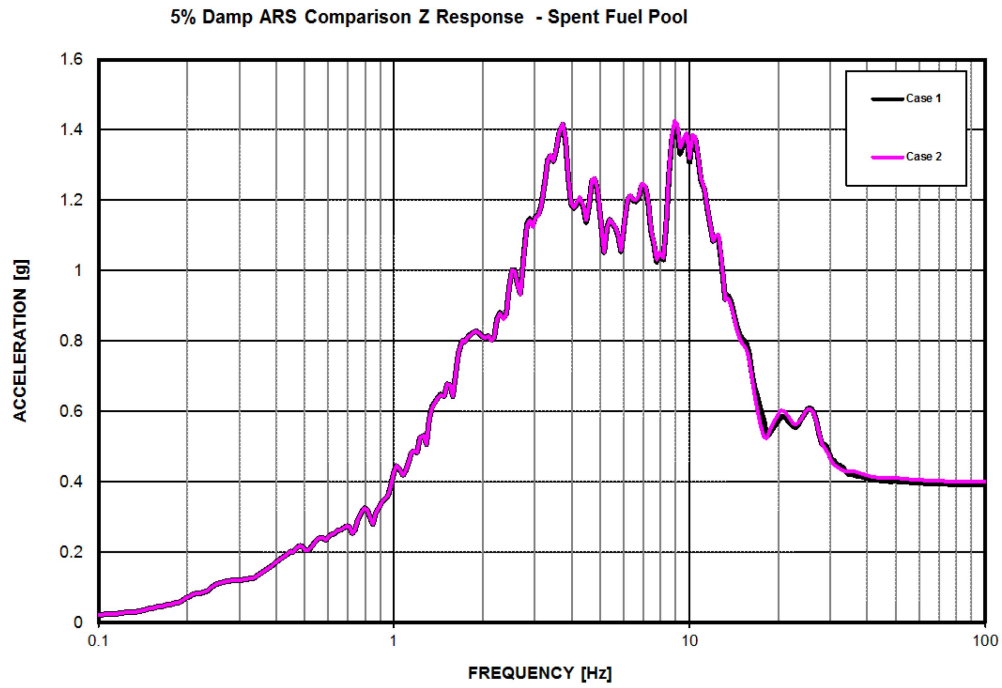


Figure 12 Response in Vertical Direction-Spent Fuel Pool

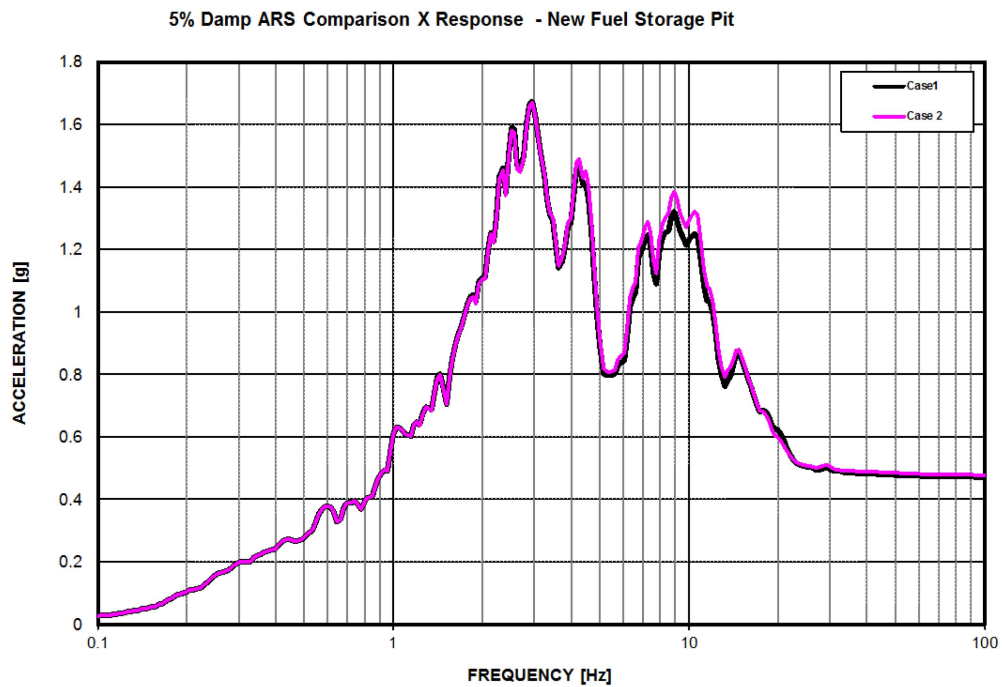


Figure 13 Response in NS Direction-New Storage Pit

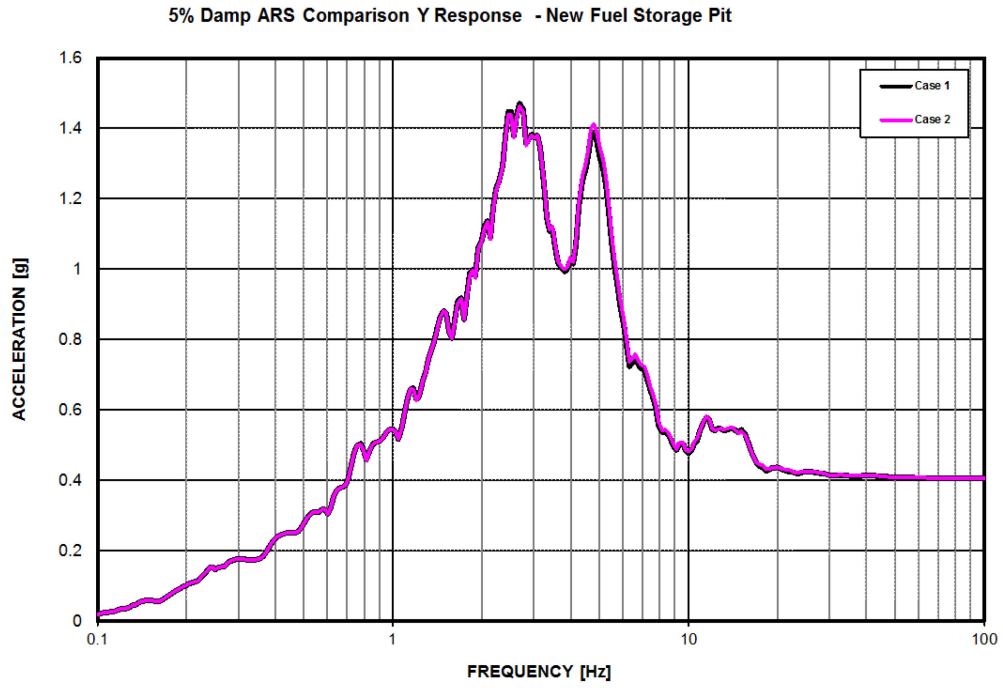


Figure 14 Response in EW Direction-New Storage Pit

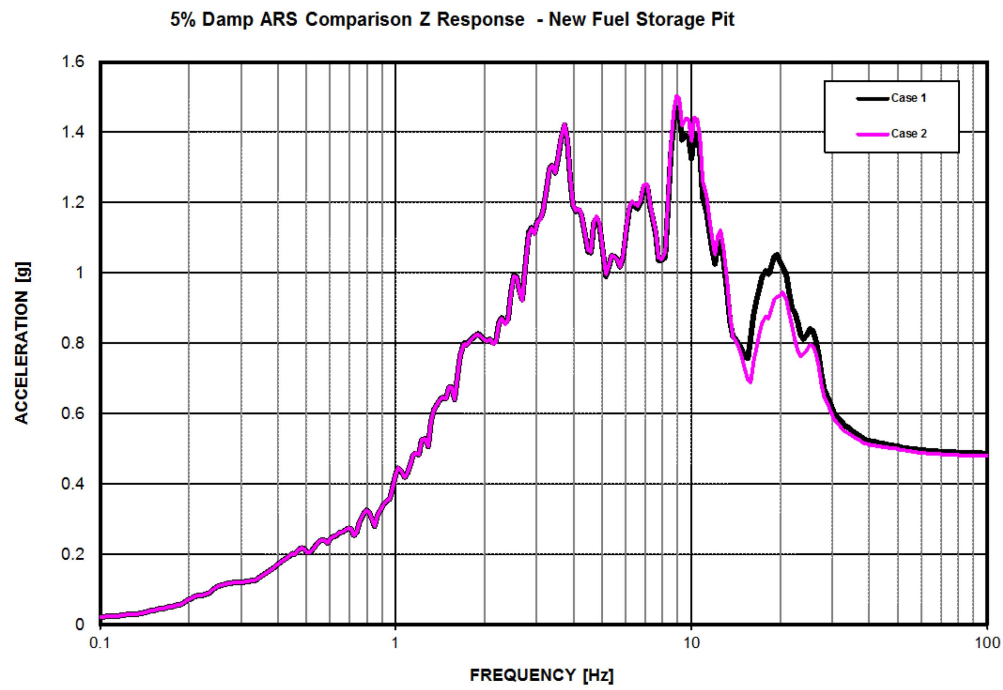


Figure 15 Response in Vertical Direction-New Storage Pit

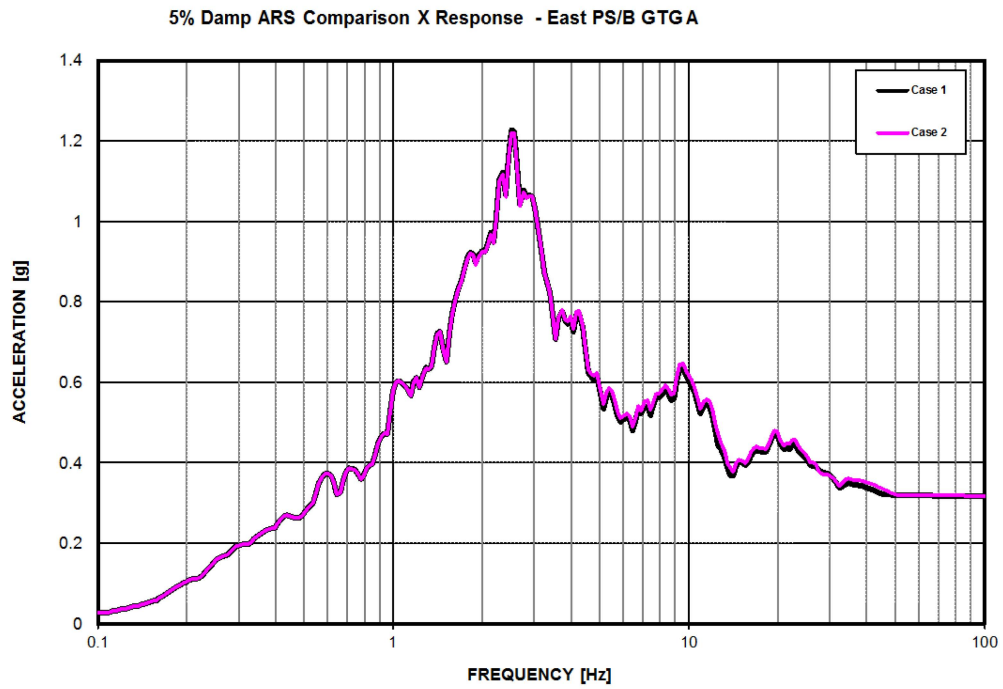


Figure 16 Response in NS Direction-East PS/B GTG A

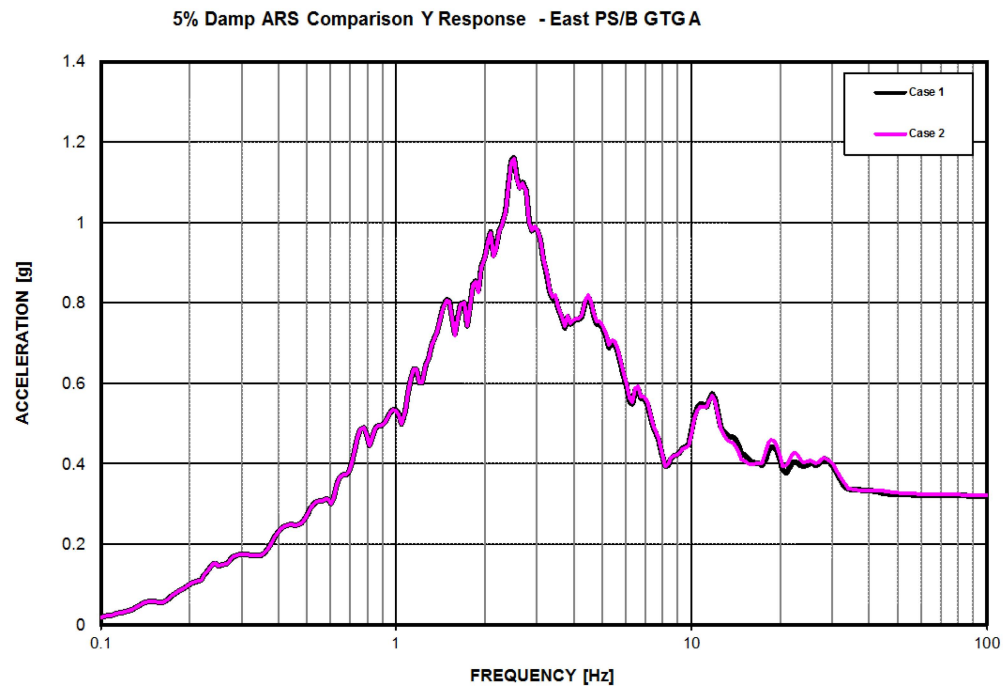


Figure 17 Response in EW Direction-East PS/B GTG A

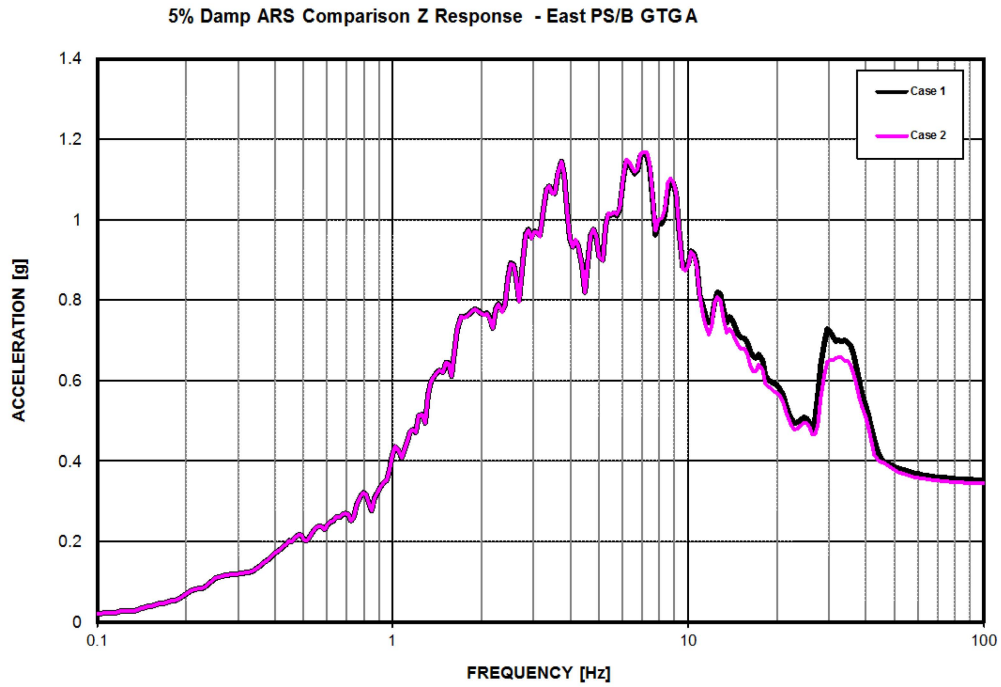


Figure 18 Response in Vertical Direction-East PS/B GTG A

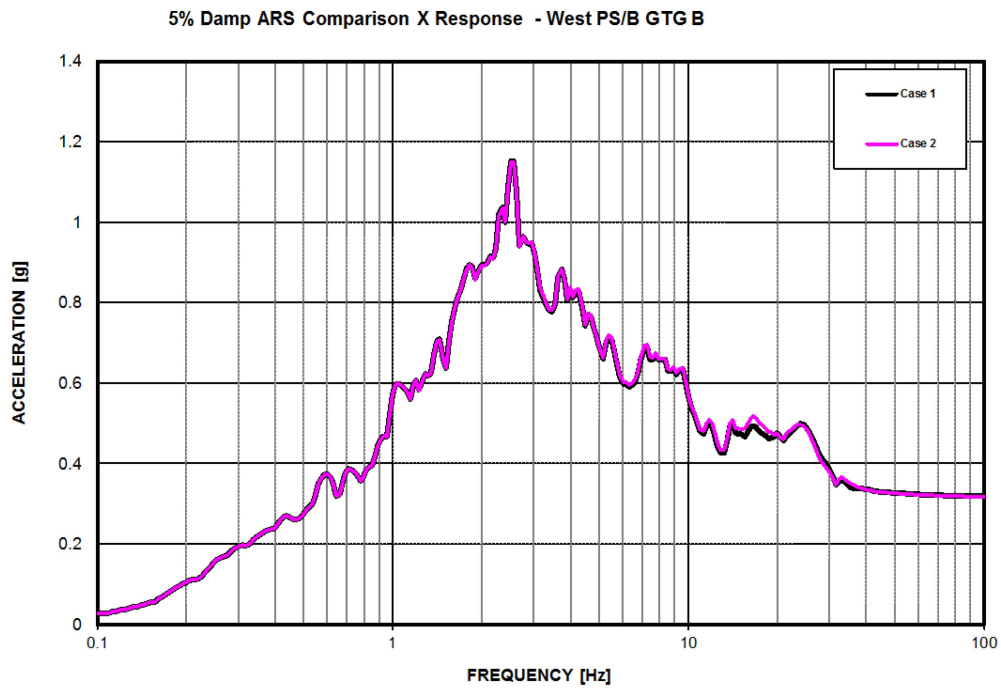


Figure 19 Response in NS Direction-West PS/B GTG B

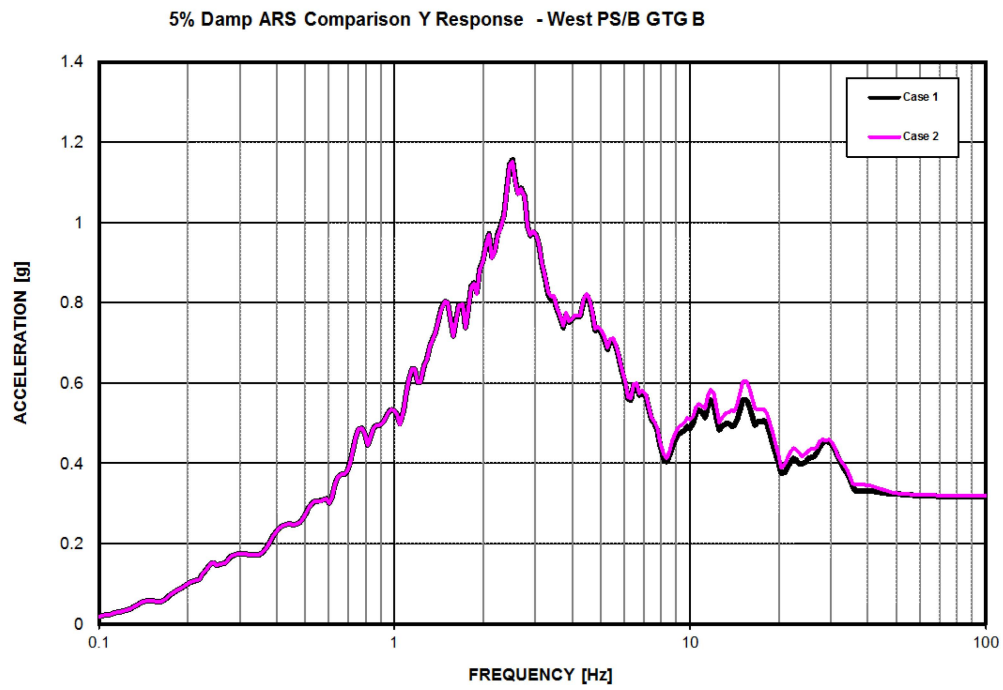


Figure 20 Response in EW Direction-West PS/B GTG B

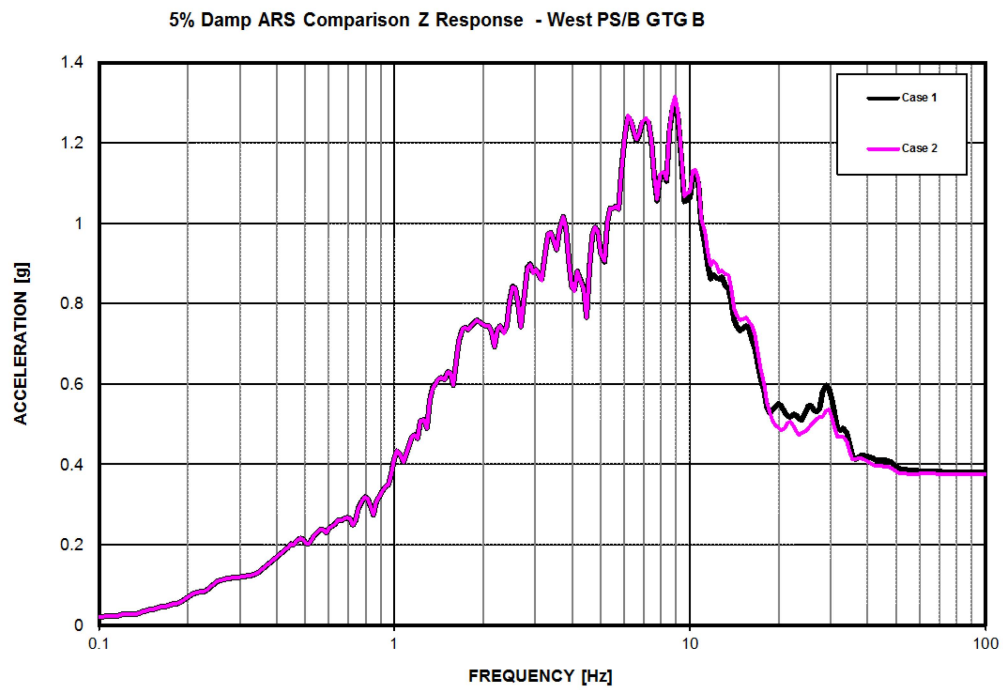


Figure 21 Response in Vertical Direction-West PS/B GTG B



Figure 22 Unbonded Model with Free Field Soils (Looking South)



Figure 23 Fully Bonded Model with Free Field Soils (Looking South)

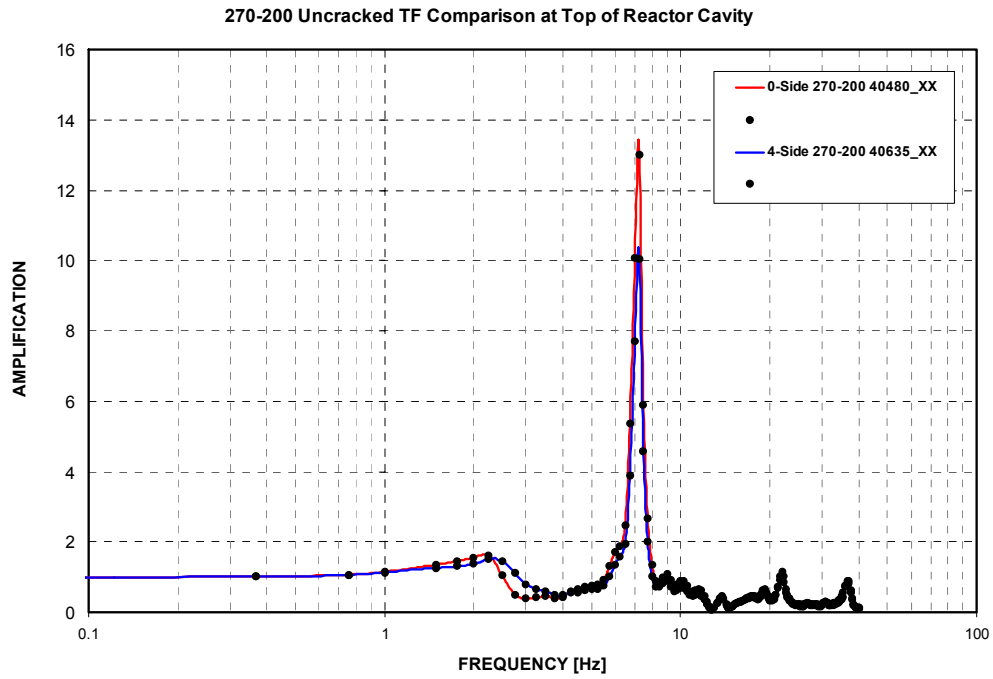


Figure 24 ATF Comparison at Top of Reactor Cavity – 270-200 – X Response

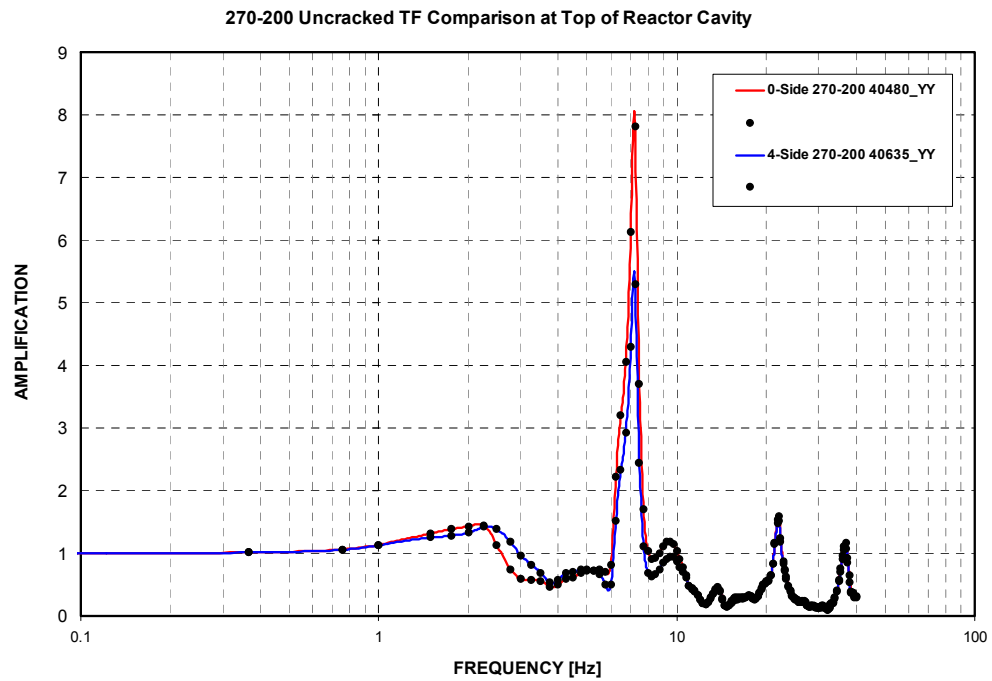


Figure 25 ATF Comparison at Top of Reactor Cavity – 270-200 – Y Response

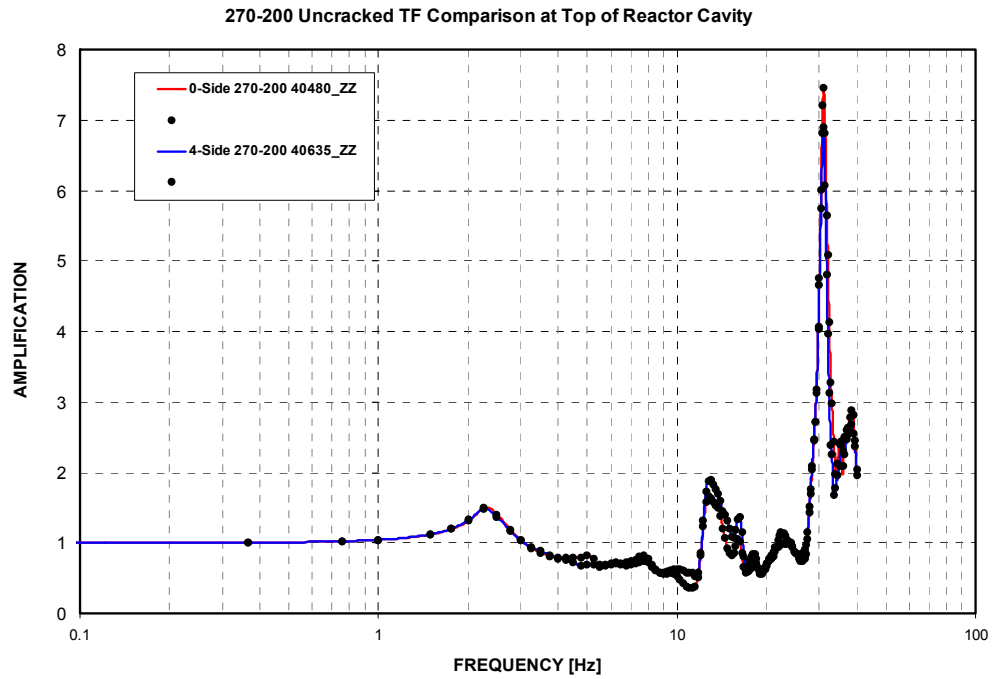


Figure 26 ATF Comparison at Top of Reactor Cavity – 270-200 – Z Response

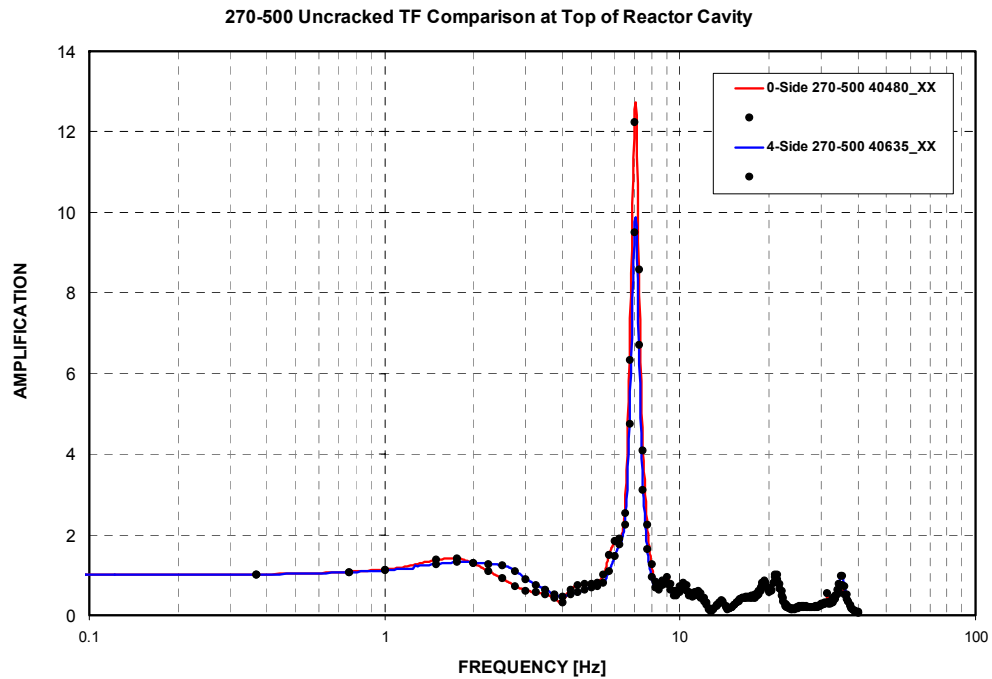


Figure 27 ATF Comparison at Top of Reactor Cavity – 270-500 – X Response

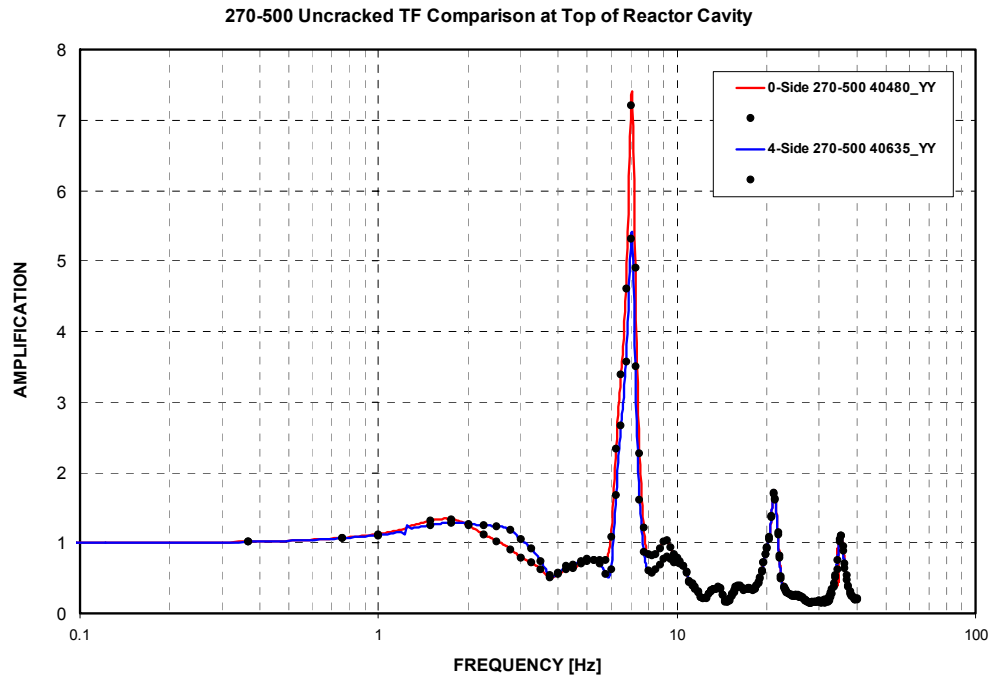


Figure 28 ATF Comparison at Top of Reactor Cavity – 270-500 – Y Response

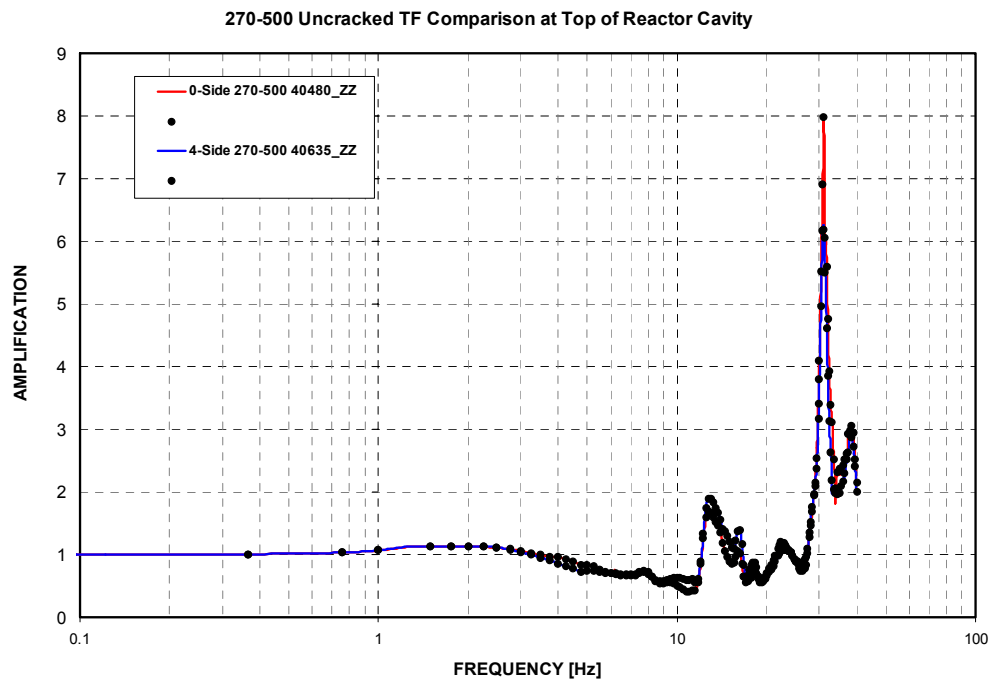


Figure 29 ATF Comparison at Top of Reactor Cavity – 270-500 – Z Response

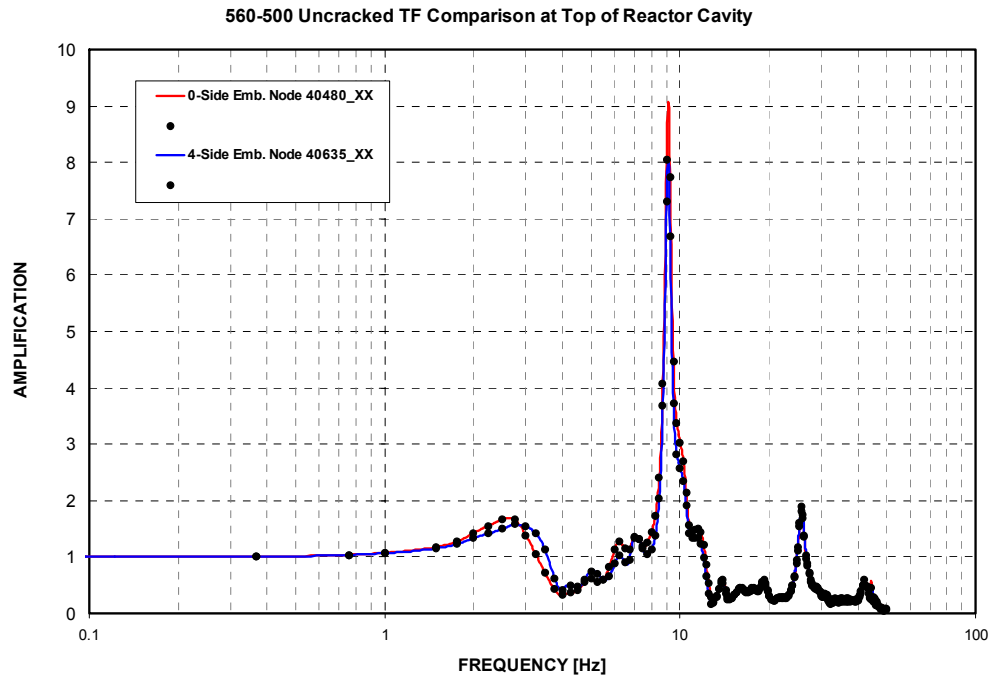


Figure 30 ATF Comparison at Top of Reactor Cavity – 560-500 – X Response

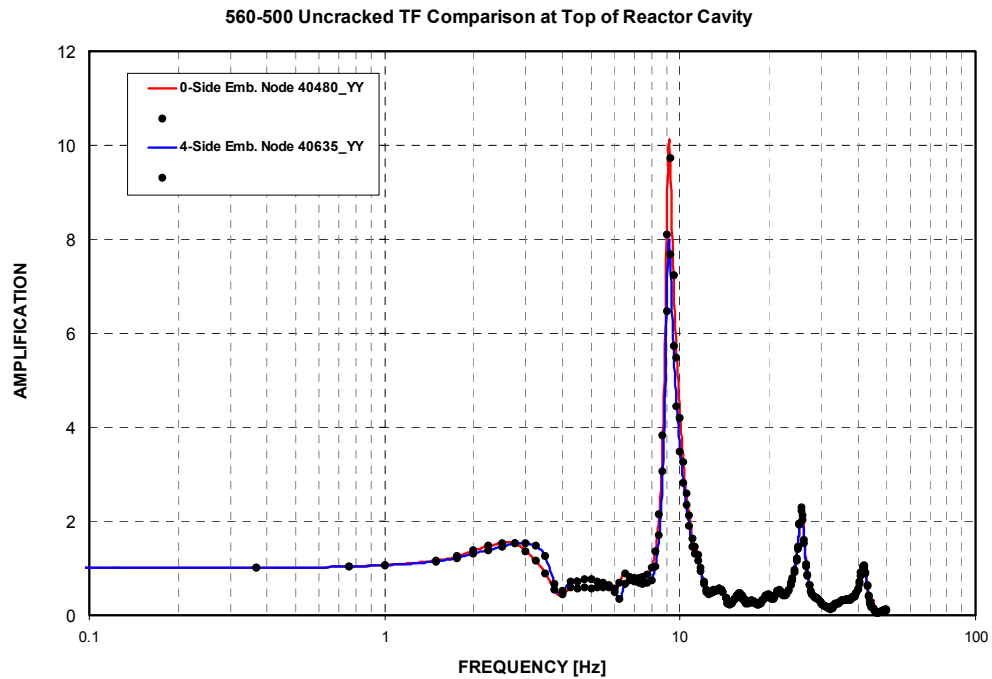


Figure 31 ATF Comparison at Top of Reactor Cavity – 560-500 – Y Response

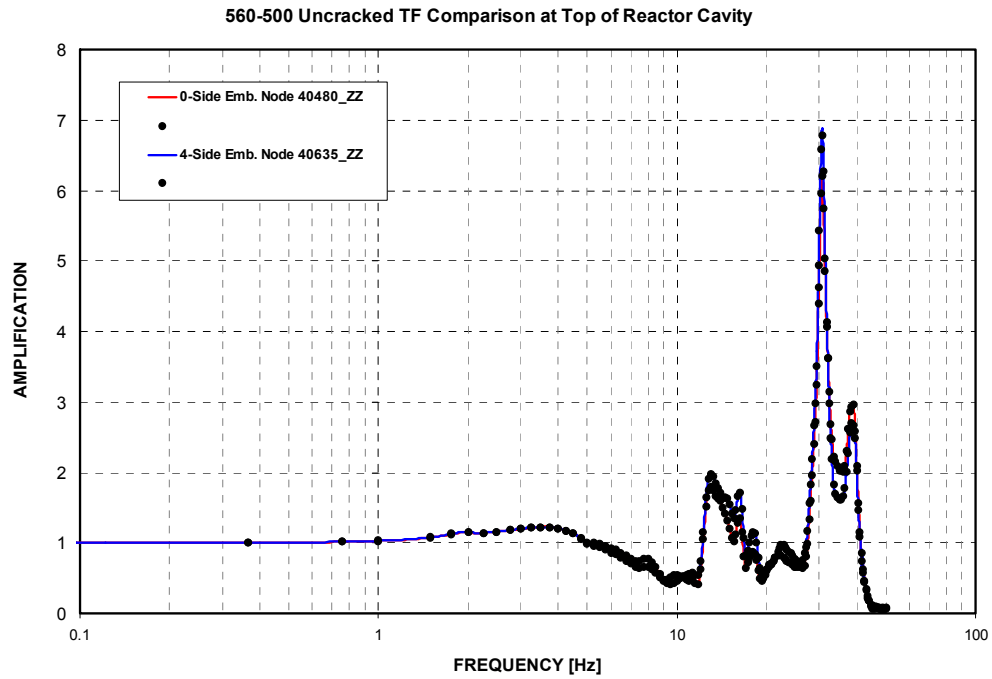


Figure 32 ATF Comparison at Top of Reactor Cavity – 560-500 – Z Response

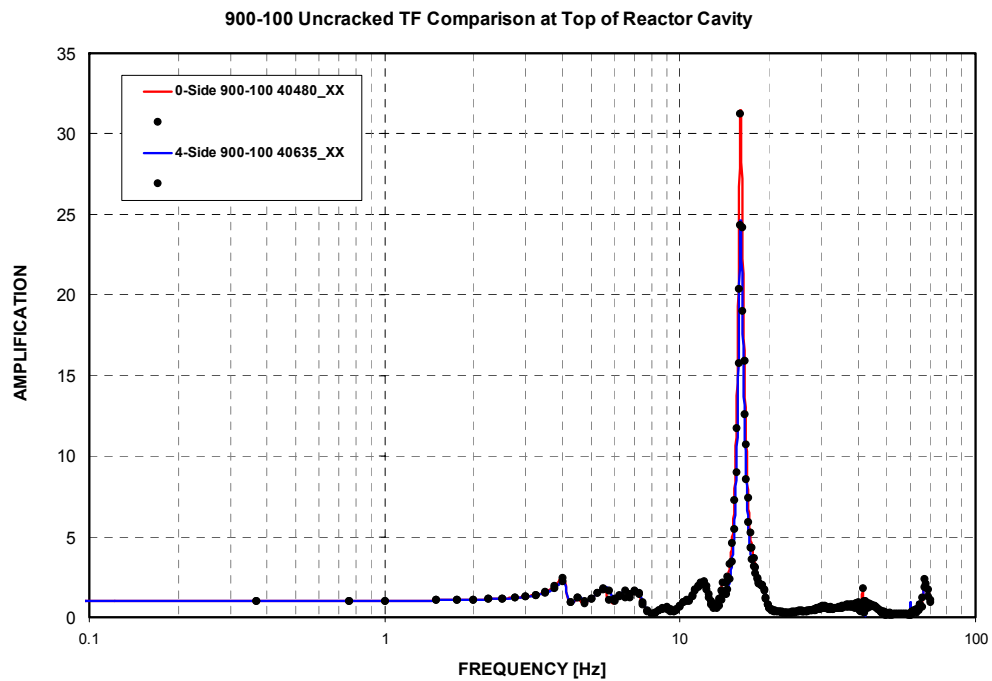


Figure 33 ATF Comparison at Top of Reactor Cavity – 900-100 – X Response

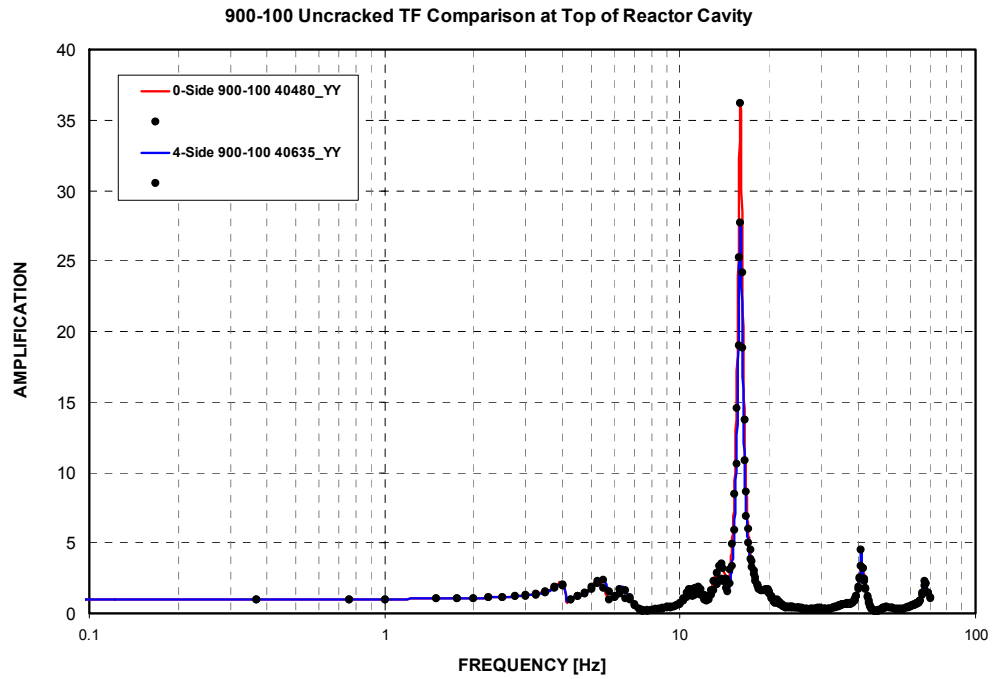


Figure 34 ATF Comparison at Top of Reactor Cavity – 900-100 – Y Response

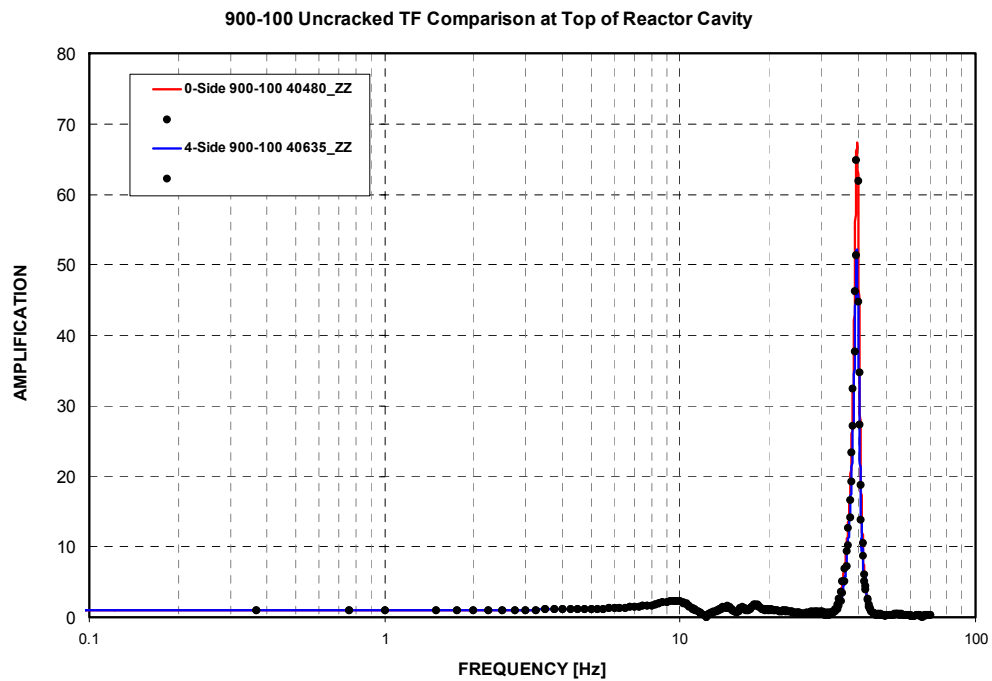


Figure 35 ATF Comparison at Top of Reactor Cavity – 900-100 – Z Response

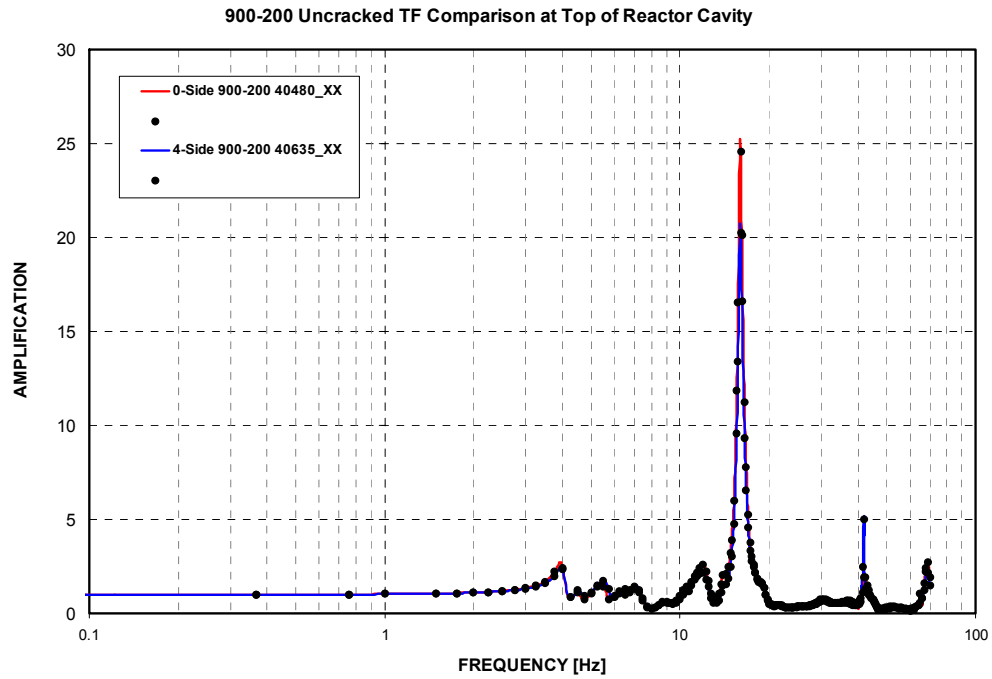


Figure 36 ATF Comparison at Top of Reactor Cavity – 900-200 – X Response

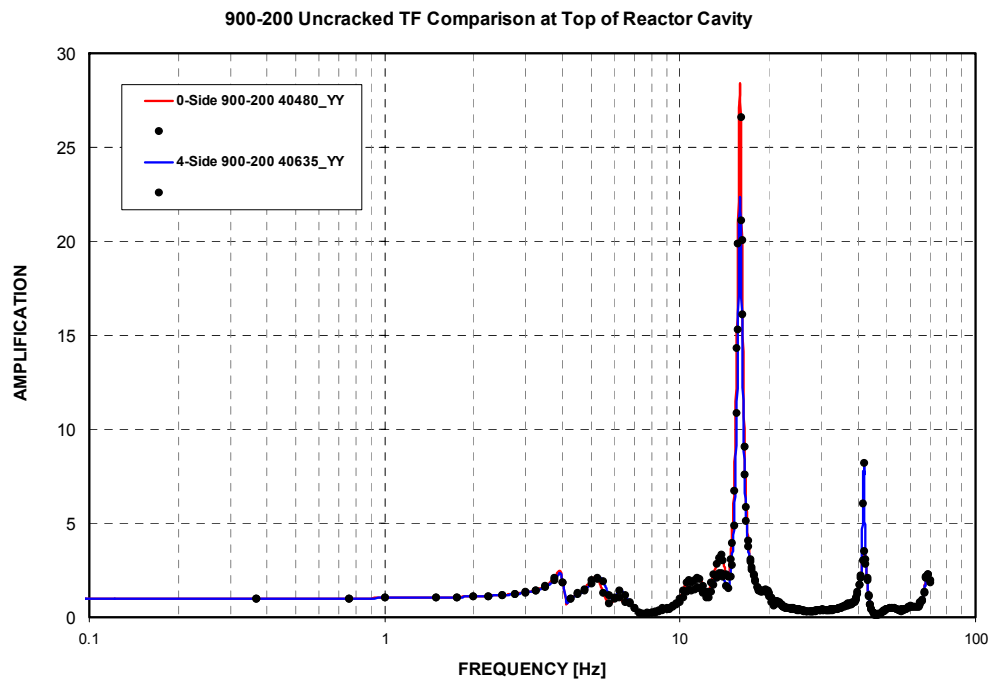


Figure 37 ATF Comparison at Top of Reactor Cavity – 900-200 – Y Response

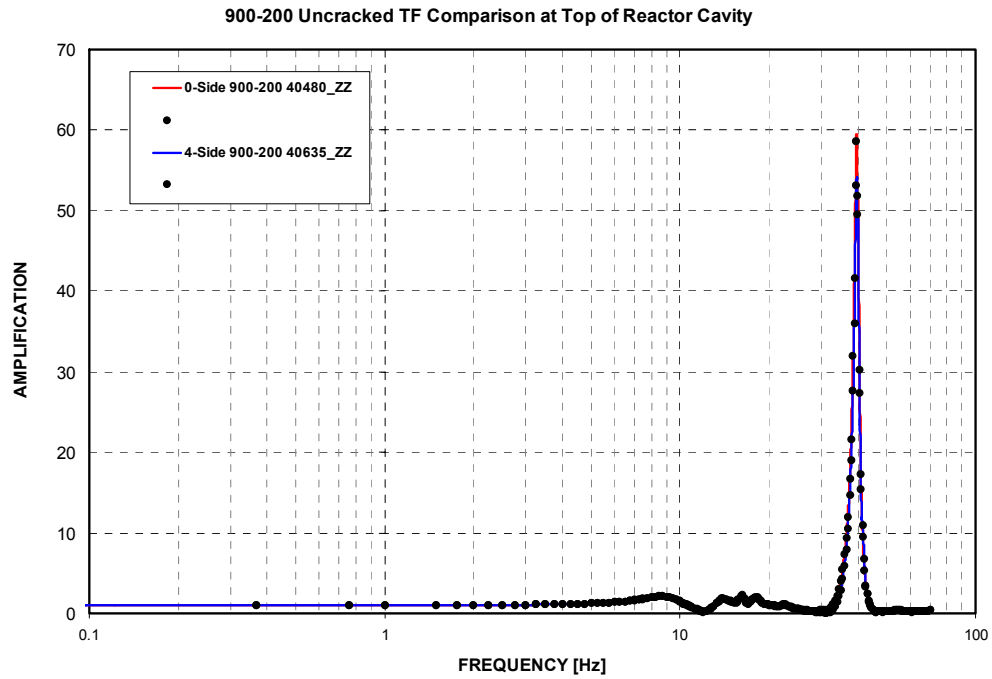


Figure 38 ATF Comparison at Top of Reactor Cavity – 900-200 – Z Response

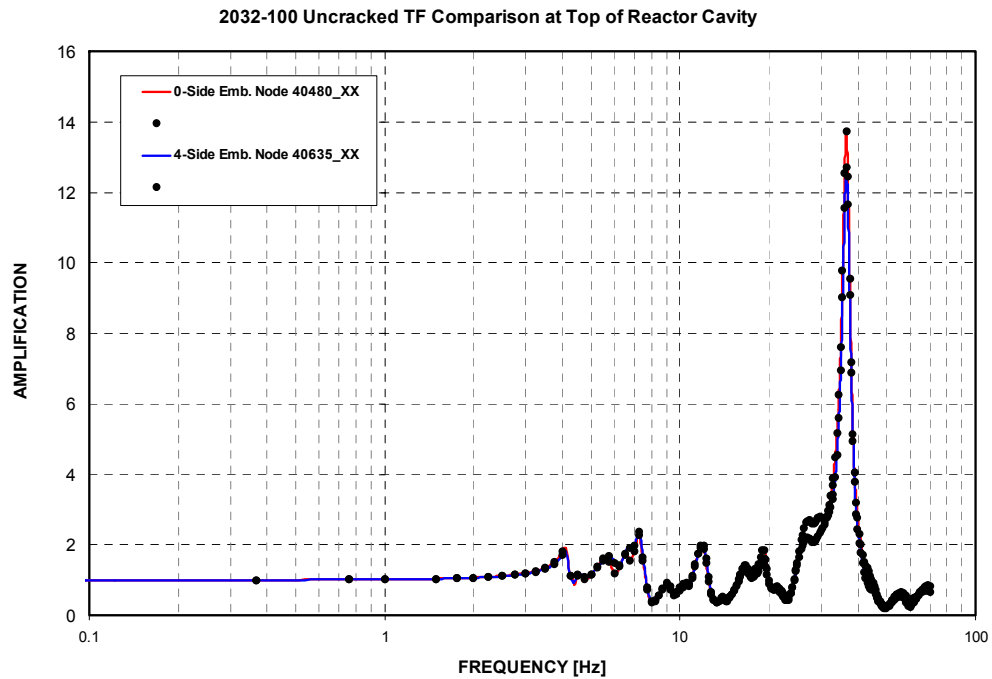


Figure 39 ATF Comparison at Top of Reactor Cavity – 2032-100 – X Response

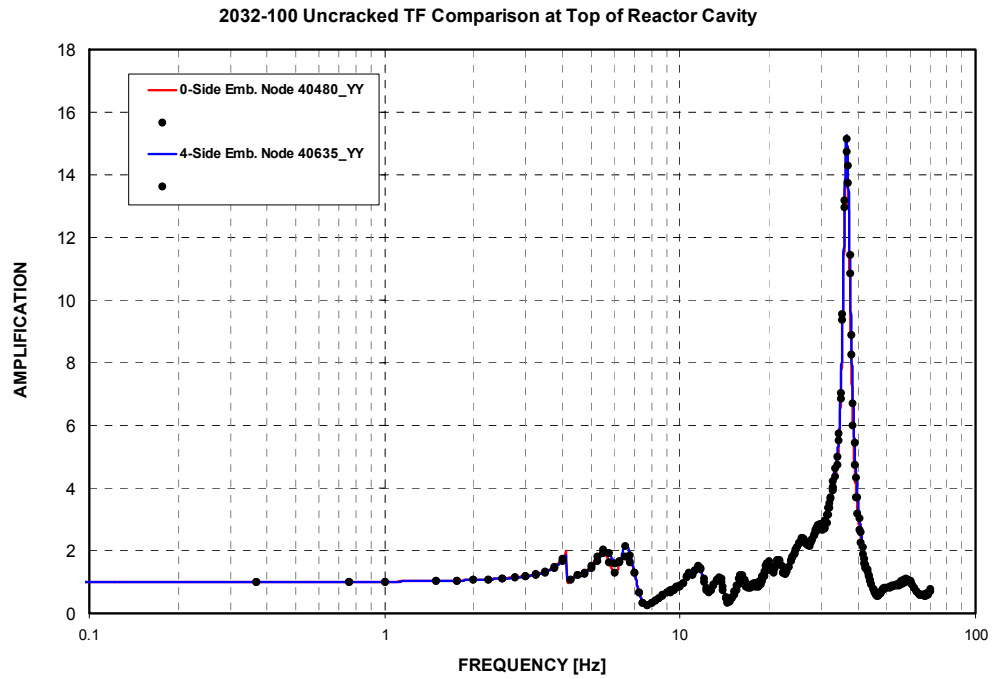


Figure 40 ATF Comparison at Top of Reactor Cavity – 2032-100 – Y Response

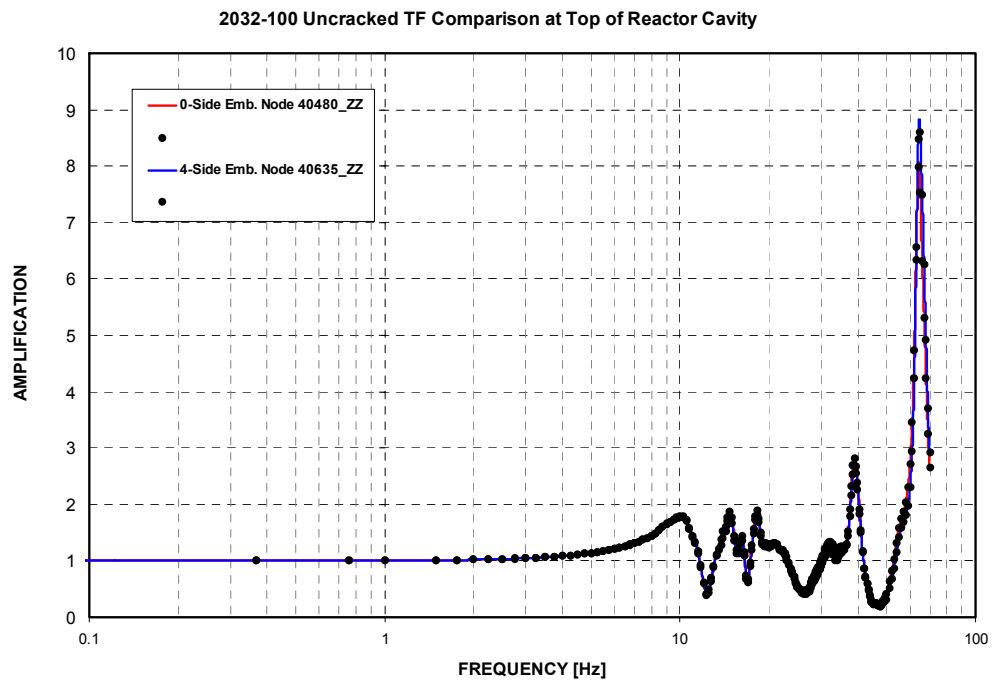


Figure 41 ATF Comparison at Top of Reactor Cavity – 2032-100 – Z Response

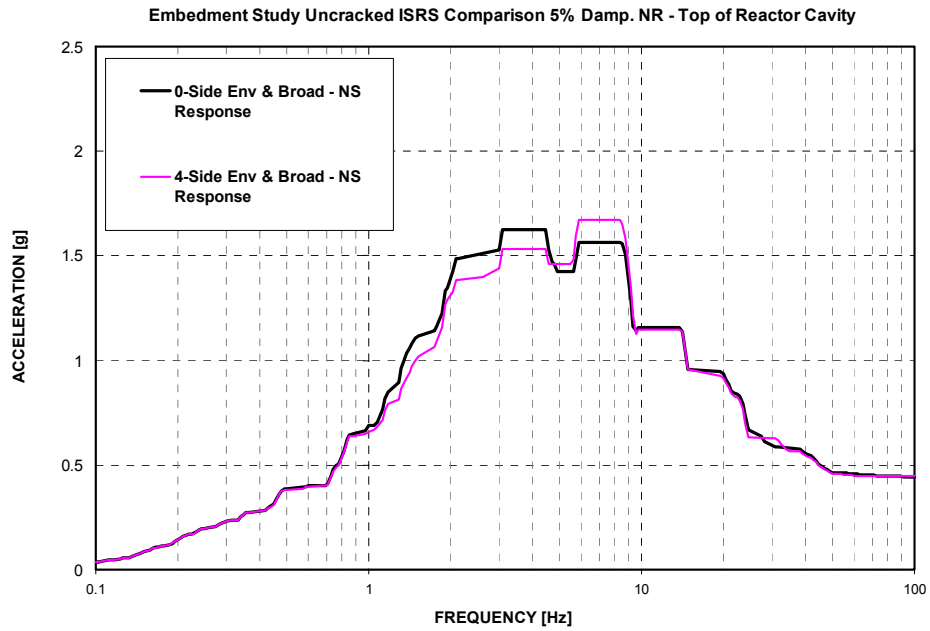


Figure 42 Top of Reactor Cavity ISRS Comparison Plot - Response in NS Direction

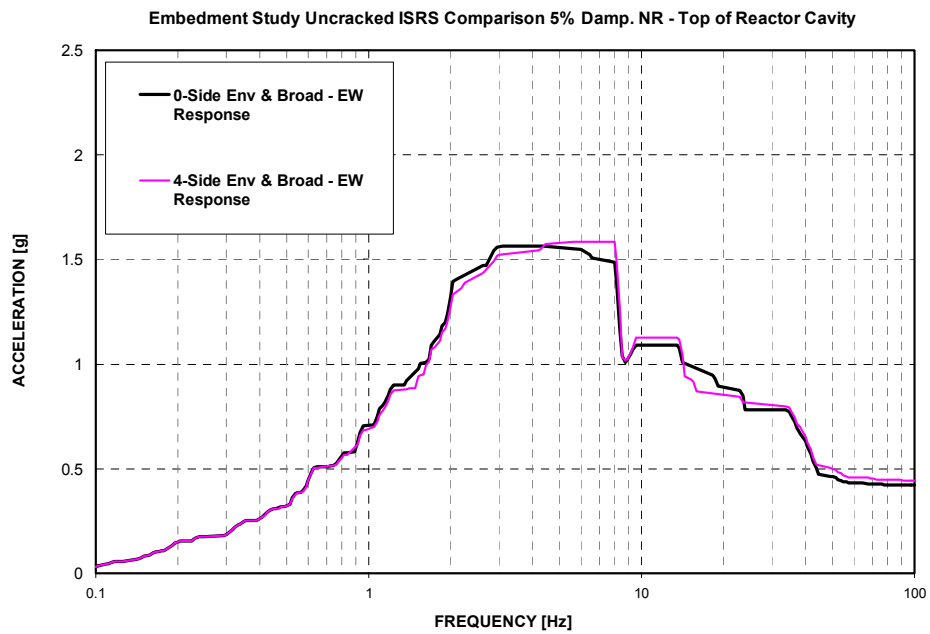


Figure 43 Top of Reactor Cavity ISRS Comparison Plot - Response in EW Direction

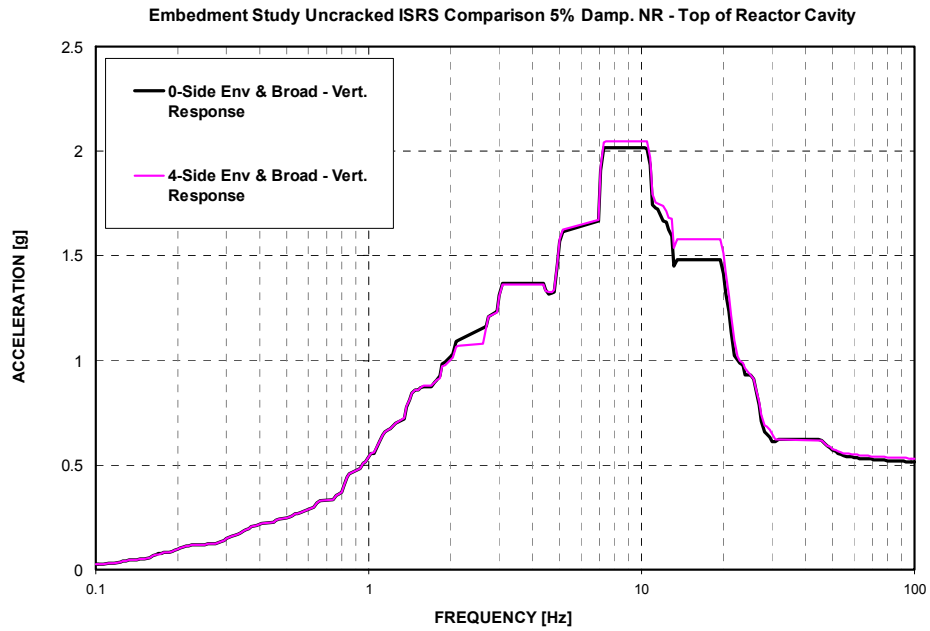


Figure 44 Top of Reactor Cavity ISRS Comparison Plot - Response in Vertical Direction

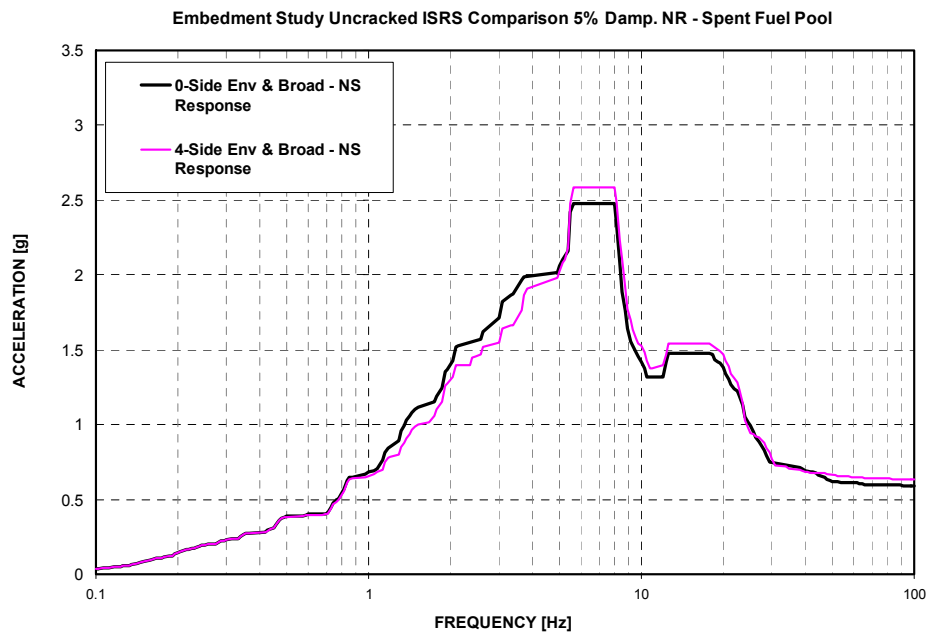


Figure 45 Spent Fuel Pool ISRS Comparison Plot - Response in NS Direction

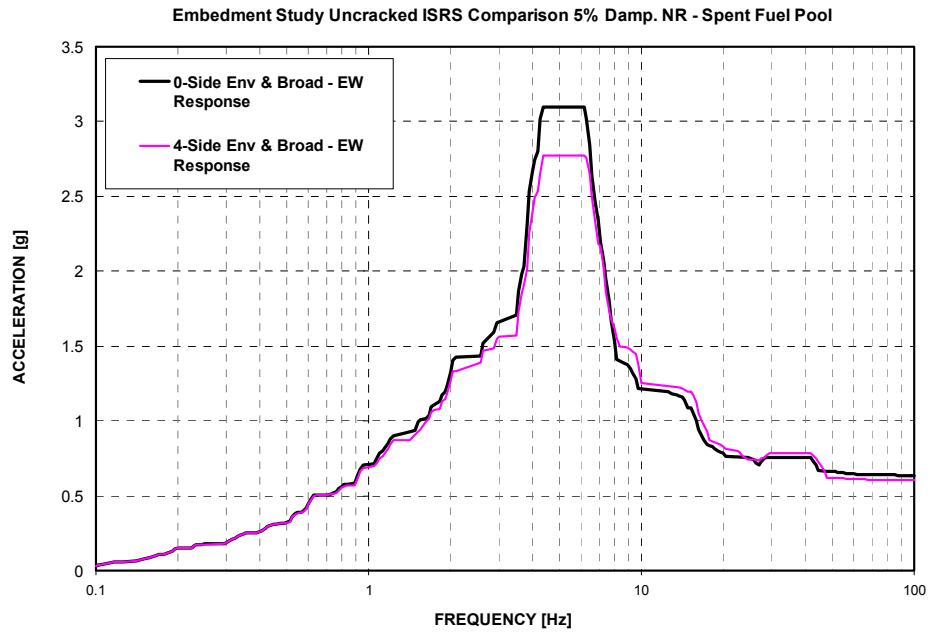


Figure 46 Spent Fuel Pool ISRS Comparison Plot - Response in EW Direction

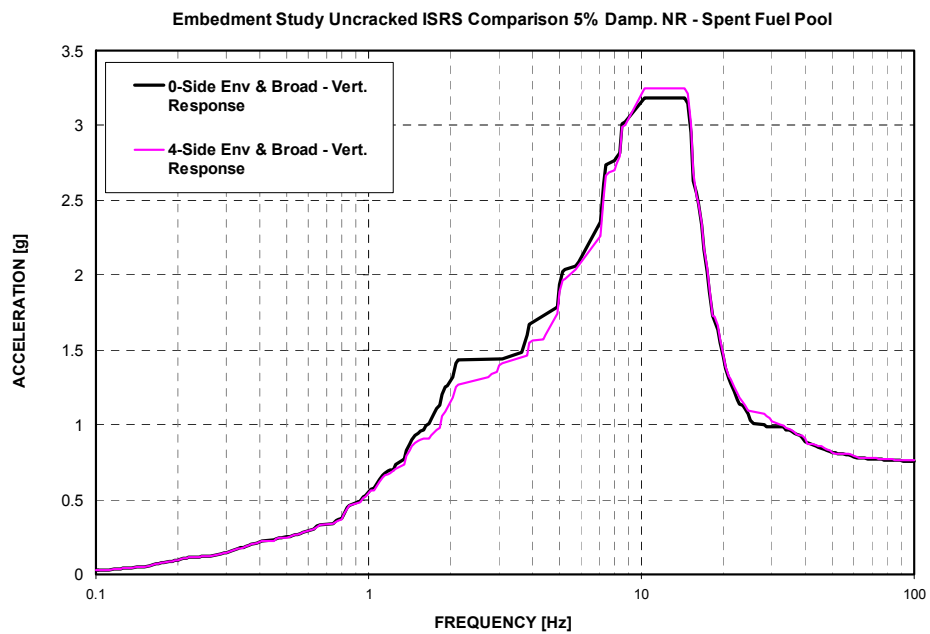


Figure 47 Spent Fuel Pool ISRS Comparison Plot - Response in Vertical Direction

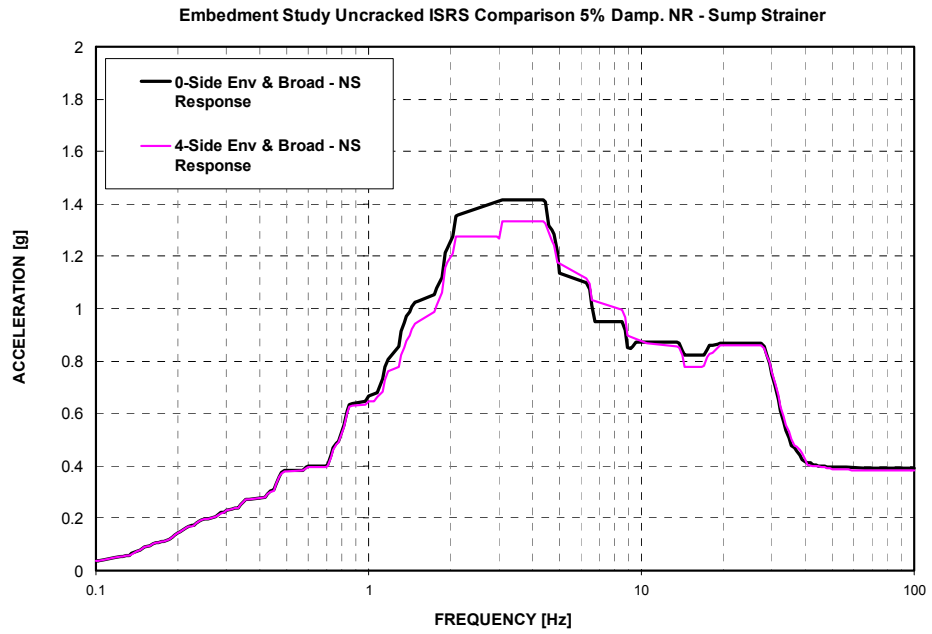


Figure 48 Sump Strainer ISRS Comparison Plot - Response in NS Direction

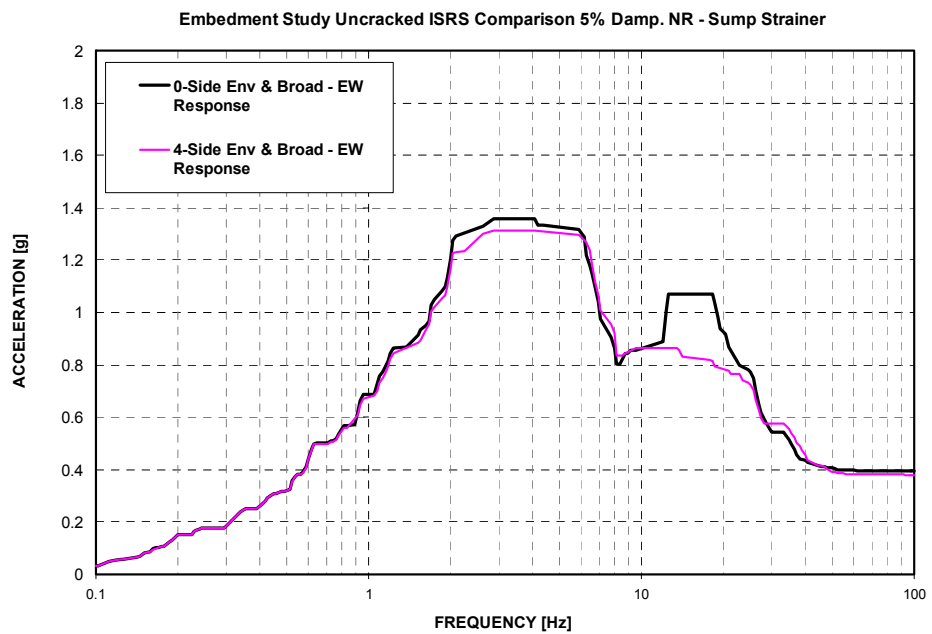


Figure 49 Sump Strainer ISRS Comparison Plot - Response in EW Direction

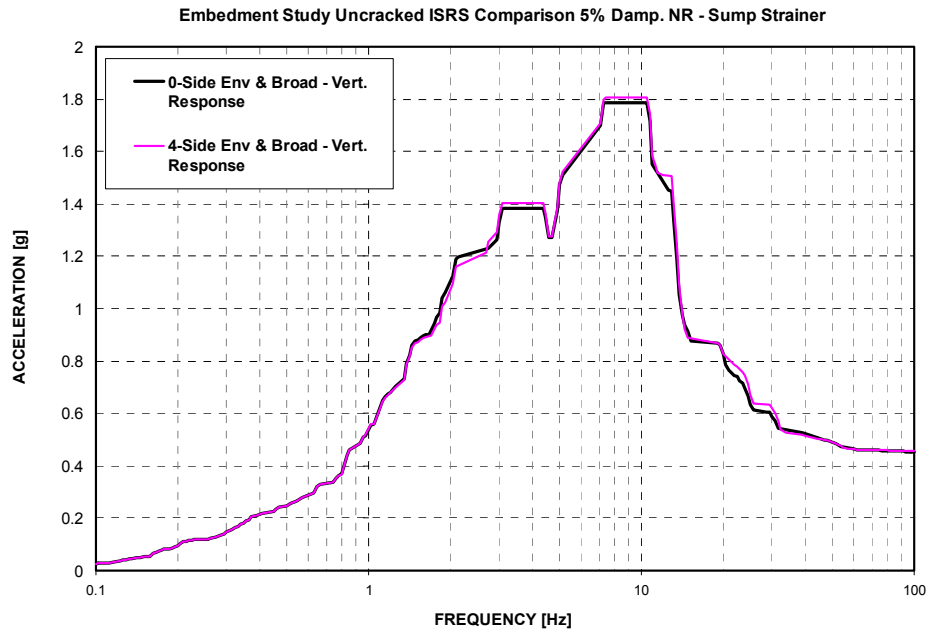


Figure 50 Sump Strainer ISRS Comparison Plot - Response in Vertical Direction

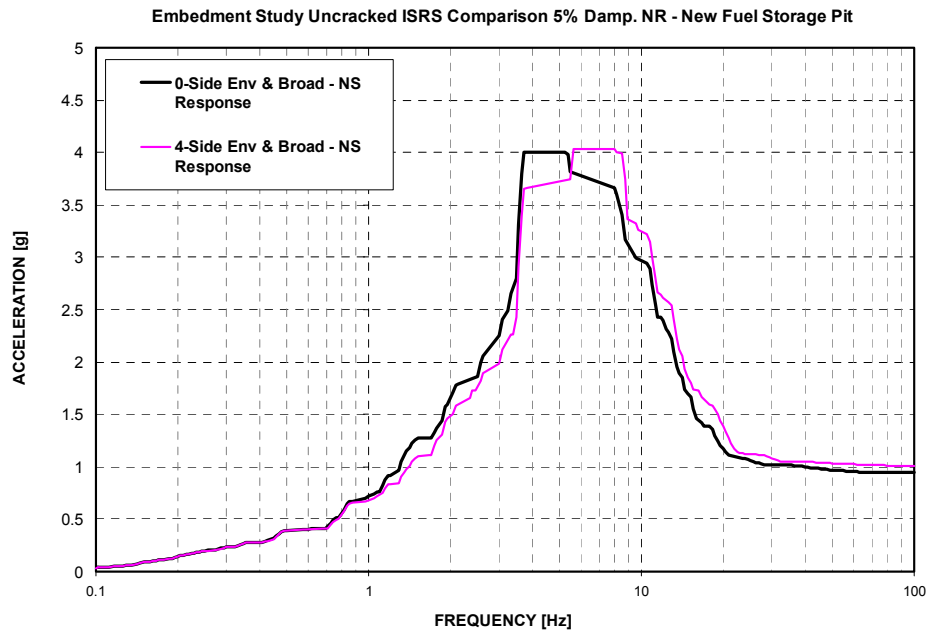


Figure 51 New Fuel Storage Pit ISRS Comparison Plot - Response in NS Direction

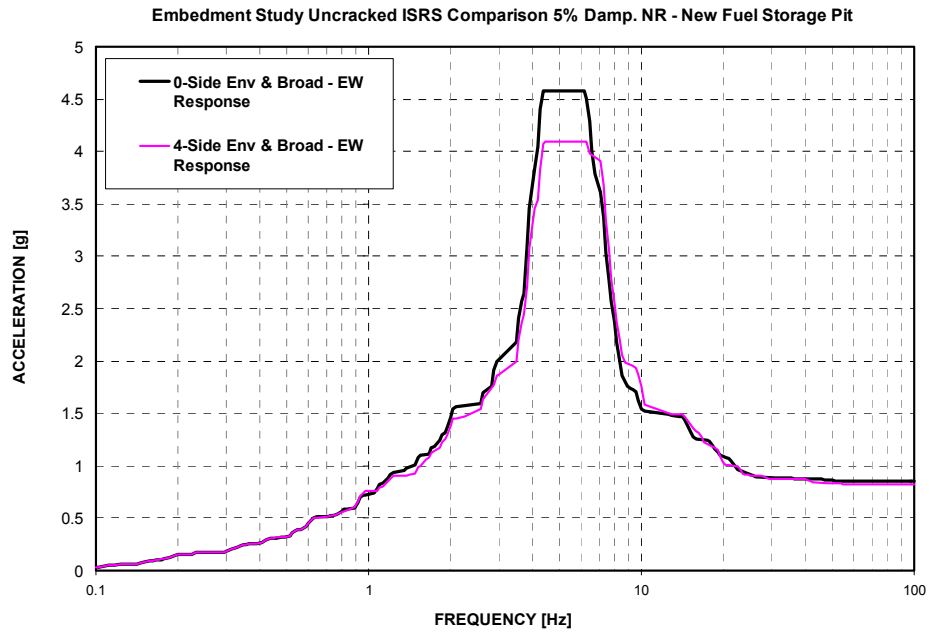


Figure 52 New Fuel Storage Pit ISRS Comparison Plot - Response in EW Direction

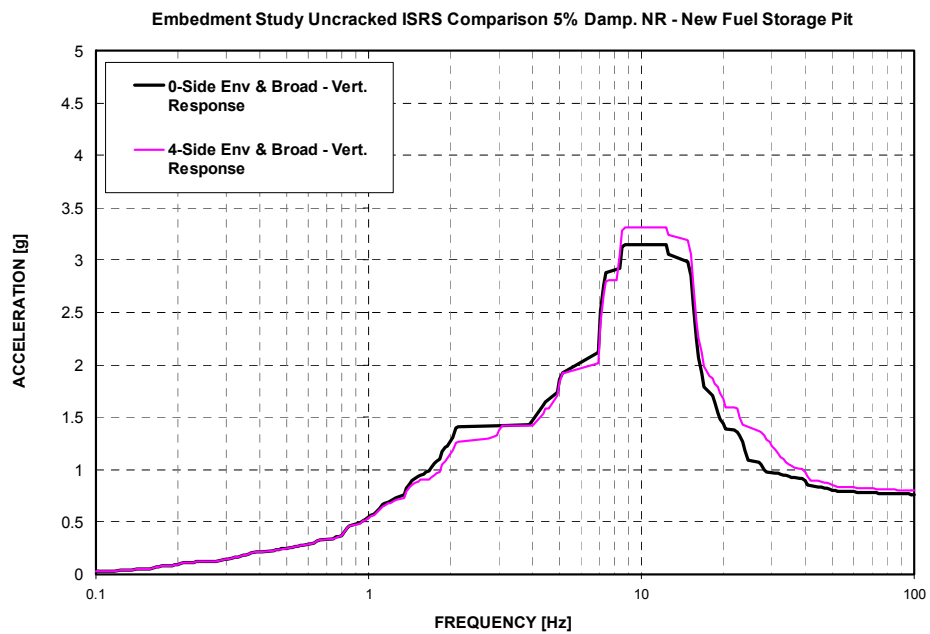


Figure 53 New Fuel Storage Pit ISRS Comparison Plot - Response in Vertical Direction

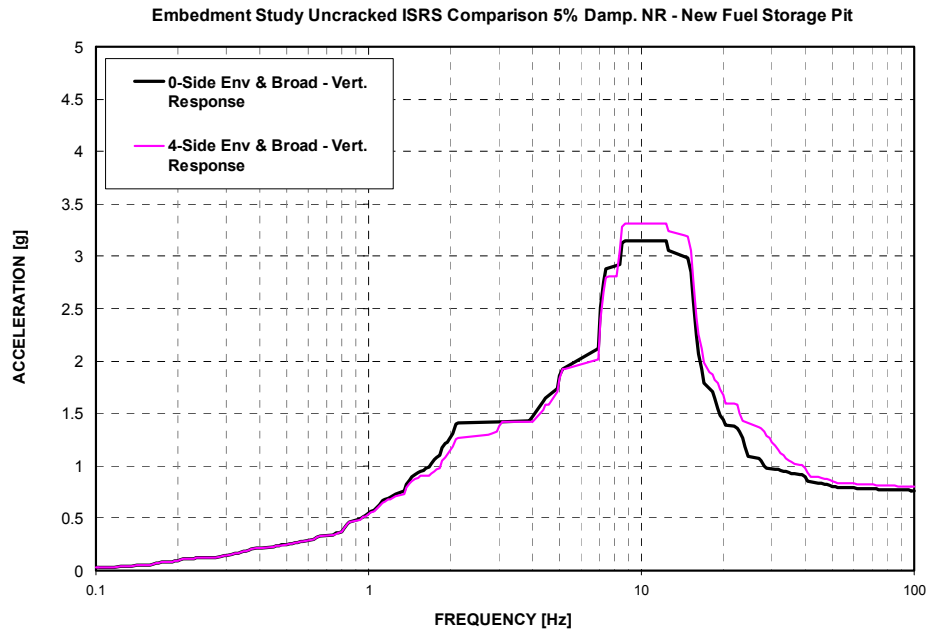


Figure 54 New Fuel Storage Pit ISRS Comparison Plot - Response in Vertical Direction - Uncracked

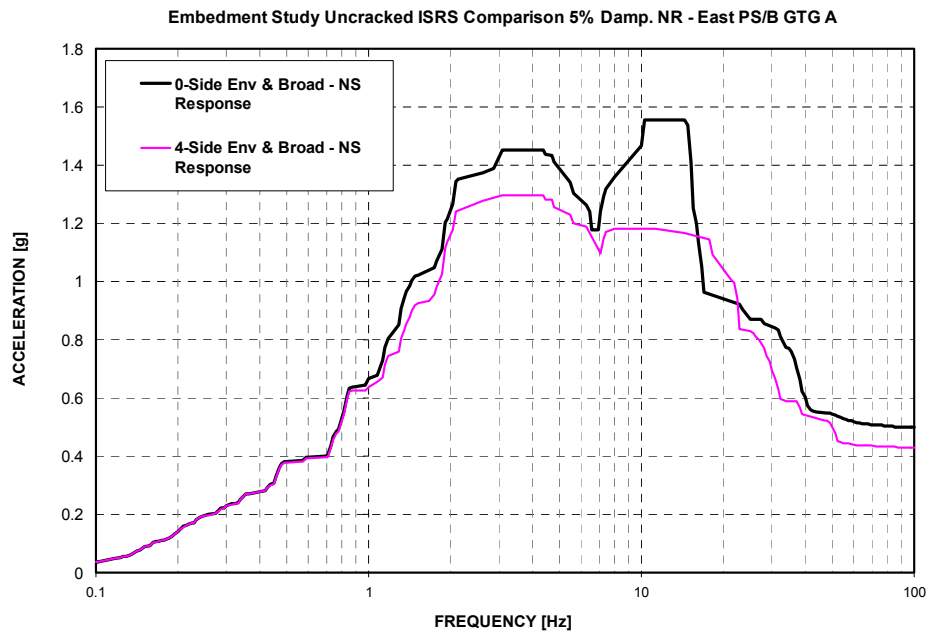


Figure 55 East PS/B GTG A ISRS Comparison Plot - Response in NS Direction

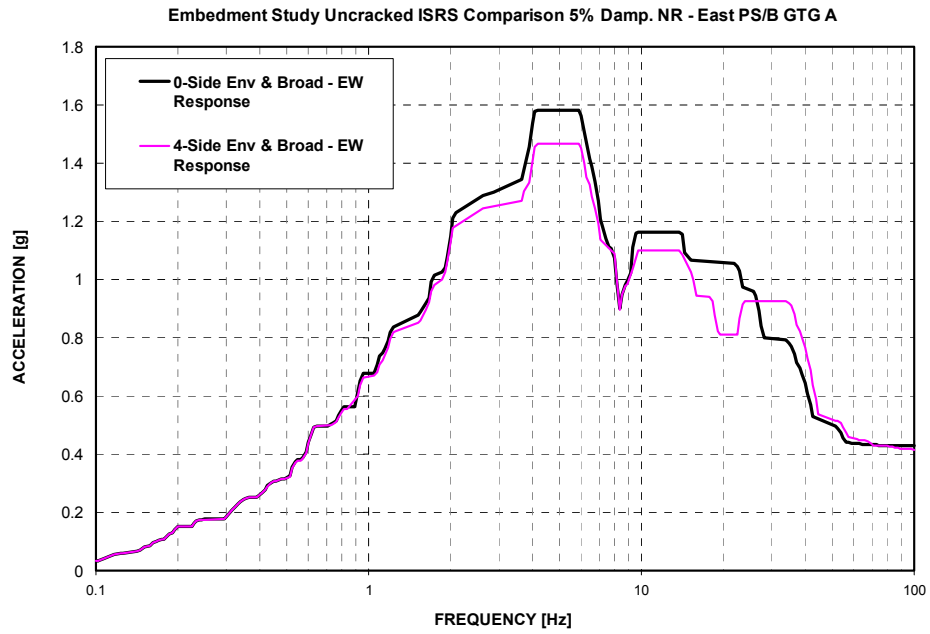


Figure 56 East PS/B GTG A ISRS Comparison Plot - Response in EW Direction

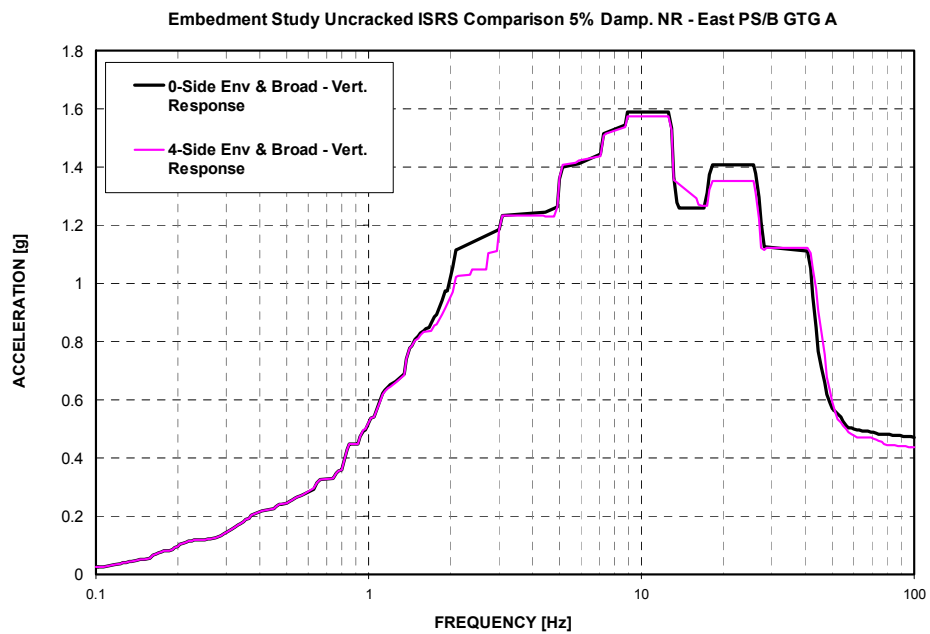


Figure 57 East PS/B GTG A ISRS Comparison Plot - Response in Vertical Direction

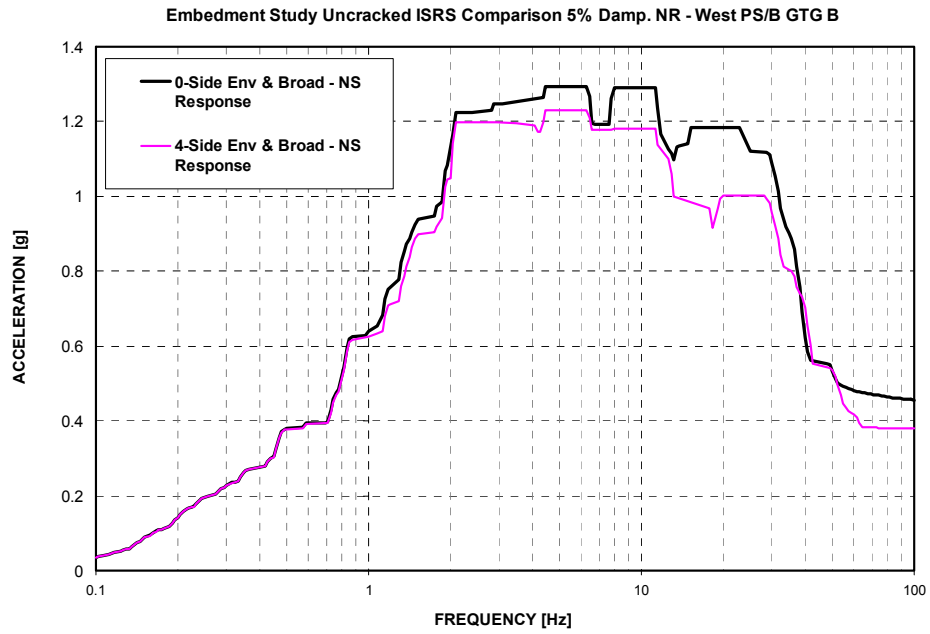


Figure 58 West PS/B GTG B ISRS Comparison Plot - Response in NS Direction

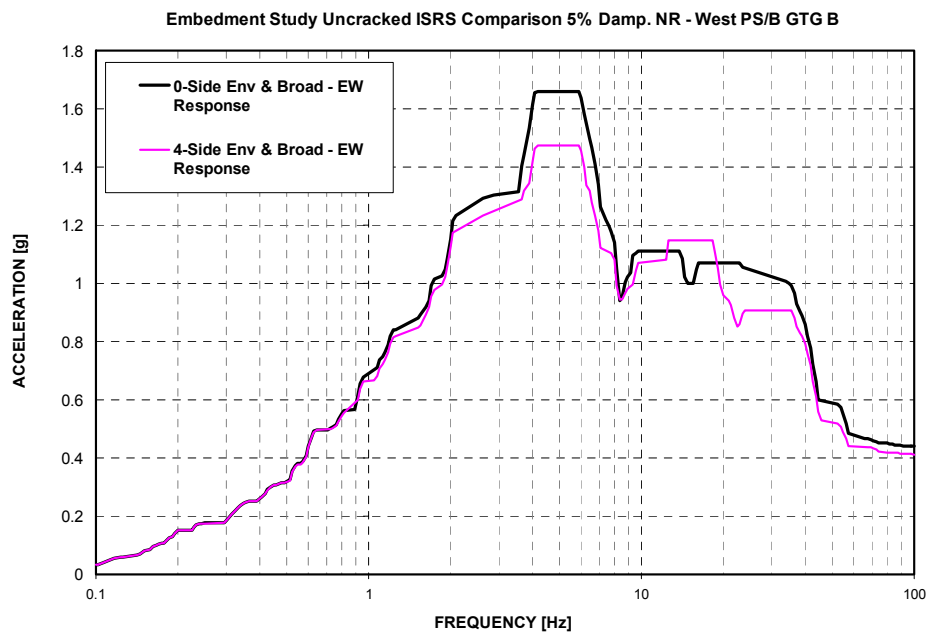


Figure 59 West PS/B GTG B ISRS Comparison Plot - Response in EW Direction

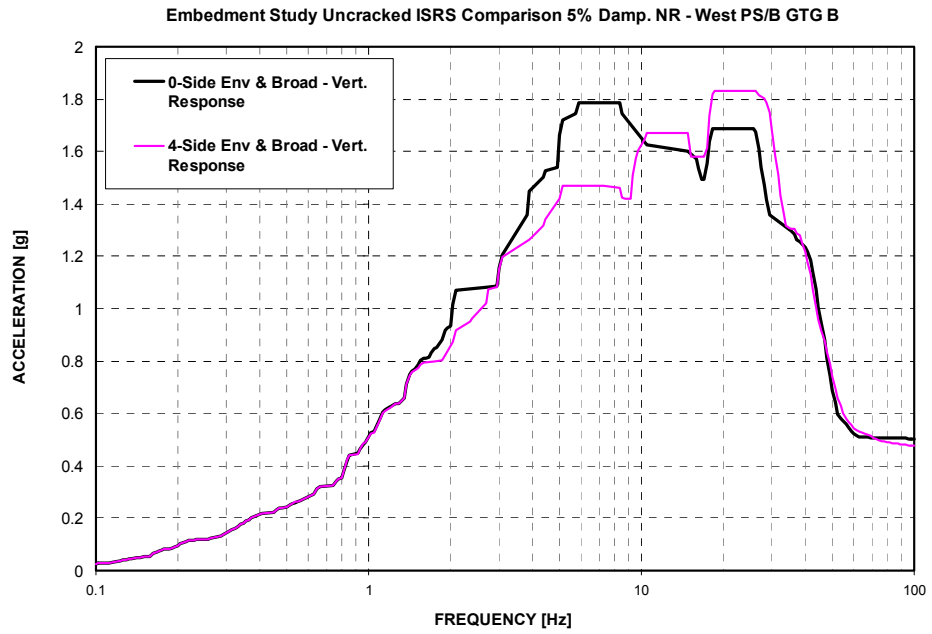


Figure 60 West PS/B GTG B ISRS Comparison Plot - Response in Vertical Direction

Impact on DCD

DCD Section 3.7 will be revised.

Impact on R-COLA

There is no impact on the R-COLA.

Impact on PRA

There is no impact on the PRA.

Impact on Technical/Topical Report

Technical Report MUAP-10006 will be revised as per discussion in Part 2 of this response.

This completes MHI's response to the NRC's question.